Functional Role of 97R in Host Cell Modulation during Frog Virus 3 Infection

A Thesis Submitted to the Committee on Graduate Studies

in Partial Fulfillment of the Requirements for the

Degree of Master of Science

in the Faculty of Arts and Science

TRENT UNIVERSITY

Peterborough, Ontario, Canada

Environmental and Life Sciences M.Sc. Graduate Program

September 2025

ABSTRACT

Functional Role of 97R in Host Cell Modulation during Frog Virus 3 Infection

Lakshika Bansal

Frog virus 3 (FV3) belongs to the genus *Ranavirus* within the *Iridoviridae* family. Its 105,903 base genome encodes 98 open reading frames (ORFs), including ORF 97R, a putative apoptosis regulator sharing 31% structural similarity with the anti-apoptotic Bcl-2 family protein, myeloid cell leukemia 1 (Mcl-1). 97R contains a BH1 domain, implicated in apoptosis regulation, and a predicted C-terminal transmembrane domain, which acts as a membrane-anchoring domain, localizing 97R to the ER membrane. To study its role in host cell modulation, 97R was cloned into a vector and transfected into HeLa cells. Immunofluorescence revealed a time-dependent decrease in Protein Disulfide Isomerase (PDI) in 97R-transfected cells. Immunoprecipitation and western blotting revealed that 97R interacts with Prohibitin 1 (PHB1), a host protein involved in apoptosis regulation. This research provides insight into the novel functional role of 97R in host cells, enhancing our understanding of how FV3 may manipulate its host.

KEYWORDS

Iridoviridae, Ranavirus, frog virus 3, ORF 97R, Bcl-2 protein family, BH1 domain, C-terminus transmembrane domain, endoplasmic reticulum, ER stress, Apoptosis, Protein disulfide isomerase, Prohibitin, Protein-protein interactions, Host cell modulation.

ACKNOWLEDGEMENTS

I am profoundly thankful to my supervisor, Dr. Craig Brunetti, for his outstanding guidance, support, and patience. His expertise and commitment were crucial to the completion of this research. I genuinely appreciate my committee members, Dr. Janet Yee and Dr. Stephanie Tobin, for their guidance, valuable insights, encouragement, and motivation. My gratitude also extends to Dr. Robert Huber, as well as Trent's outstanding lab instructors, Smolly Coulson and Debbie Lietz, for generously allowing me to use their lab equipment and providing technical support.

I am grateful to Dr. Leslie Kerr for nurturing my critical thinking, building my confidence, and developing my research skills during my undergraduate thesis at Trent. Those skills significantly aided my Master's work. I also thank Galair Prevost for constant encouragement and support. I thank the members of the Brunetti, Huber and Tobin labs for their collaboration, guidance, and shared dedication to research. My sincere gratitude goes to the staff at Lady Eaton College and Trent International, whose kindness and encouragement inspired me to pursue my goals.

Finally, I thank God, my parents, and Rachit for providing me strength during difficult times and humility during moments of success. I proudly dedicate this thesis to my mother, my first mentor, whose wisdom, unwavering support, and inspiration have shaped my journey. I am also grateful to my friends for their love and encouragement throughout my time at Trent.

TABLE OF CONTENTS

LIST OF FIGURES

LIST OF ABBREVIATIONS

APAF1	Apoptotic Protease-Activating Factor 1
ATCC	American Type Culture Collection
ATF6	Activating Transcription Factor 6
BAD	Bcl-2 Associated Agonist of Cell Death
BAK	Bcl-2 Antagonist/Killer
BAX	Bcl-2 Associated X Protein
Bcl-2	B-cell lymphoma 2
Bcl-XL	B-cell lymphoma-extra large
Bcl-XS	Bcl-2 Extra Short
BH	Bcl-2 Homology (domain)
BID	BH3 Interacting Domain Death Agonist
BiP	Binding Immunoglobulin Protein
BIM	Bcl-2 Interacting Mediator of Cell Death
BIK	Bcl-2 Interacting Killer
BLASTP	Basic Local Alignment Search Tool for Proteins
BSA	Bovine Serum Albumin
Ca^{2+}	Calcium Ion
CHOP	C/EBP Homologous Protein
CMV	Cytomegalovirus
CGSIV	Chinese Giant Salamander Iridovirus
Cy5	Cyanine5
DAPI	4′,6-Diamidino-2-Phenylindole
DMEM	Dulbecco's Modified Eagle’s Medium
Drp1	Dynamin-Related Protein 1
dsDNA	Double-Stranded DNA
DTT	Dithiothreitol
ECL	Enhanced Chemiluminescence
EGFP	Enhanced Green Fluorescent Protein
ER	Endoplasmic Reticulum

FBS	Fetal Bovine Serum
FITC	Fluorescein Isothiocyanate
FPV039	Fowlpox Virus Protein 039
FV3	Frog virus 3
GIV	Grouper Iridovirus
HRP	Horseradish Peroxidase
IgG	Immunoglobulin G
IP	Immunoprecipitation
IRE1α	Inositol-Requiring Enzyme 1 Alpha
kDa	Kilodalton
LB	Luria Bertani
Mcl-1	Myeloid Cell Leukemia 1
MHC	Major Histocompatibility Complex
MERCs	Mitochondria-Endoplasmic Reticulum Contact Sites
MOMP	Mitochondrial Outer Membrane Permeabilization
NaCl	Sodium Chloride
NCBI	National Center for Biotechnology Information
NIH3T3	Mouse Embryonic Fibroblast Cell Line
NP-40	Nonidet P-40 (a non-ionic surfactant)
ORF	Open Reading Frame
PBS	Phosphate-Buffered Saline / Predicted Biological Score (Y2H context)
PDIA6	Protein Disulfide Isomerase Associated 6
PDI	Protein Disulfide Isomerase
PERK	PKR-like Endoplasmic Reticulum Kinase
PHB1	Prohibitin 1
PHB2	Prohibitin 2
PKR	Protein Kinase R (double-stranded RNA-activated protein kinase R)
PUMA	p53 Upregulated Modulator of Apoptosis
RPM	Revolutions Per Minute
RNA	Ribonucleic Acid
SCRaV	Soft-Shelled Turtle Iridovirus

SDS	Sodium Dodecyl Sulfate
SDS-PAGE	Sodium Dodecyl Sulfate-Polyacrylamide Gel Electrophoresis
S1P	Site-1 Protease
S2P	Site-2 Protease
STIV	Singapore Grouper Iridovirus
TBST	Tris-Buffered Saline with Tween-20
TFV	Tiger Frog Virus
Tris-HCl	Tris(hydroxymethyl) aminomethane Hydrochloride
UPR	Unfolded Protein Response
vBcl-2	Viral B-cell lymphoma 2-like protein
VDAC2	Voltage-Dependent Anion Channel 2
XBP1	X-box Binding Protein 1
XBP1s	Spliced X-box Binding Protein 1
Y2H	Yeast Two-Hybrid

CHAPTER 1

GENERAL INTRODUCTION

Viruses have a significant impact on ecological systems, the health of organisms, and cellular functions. To survive within host cells, viruses have developed advanced strategies that manipulate host cellular machinery for genome replication, virion assembly, and spreading to nearby cells (Marques et al., 2024). These tactics enable viruses to modify host pathways, evade immune detection, and reprogram essential cellular functions (Marques et al., 2024). Unlike typical cellular proteins, viral proteins are often produced in large amounts and tend to be multifunctional, structurally complex, and prone to misfolding or aggregation (Marques et al., 2024). Therefore, viruses do not rely solely on the host's protein-folding machinery; they actively manipulate it (Marques et al., 2024). Many viruses affect the expression, activity, and localization of molecular chaperones and ER-resident proteins in the host cell, allowing them to alter the protein folding environment in ways that promote efficient viral replication (Aviner & Frydman, 2019). This places a unique burden on the proteostasis machinery of the host cell in the endoplasmic reticulum (ER).

ER Stress and Unfolded Protein Response in Viral Infections

The ER is a crucial site for protein synthesis, especially for membrane proteins and those exported from the cell. It plays a significant role in protein folding, lipid synthesis, and calcium storage (Fu et al., 2021). It also plays a crucial role in sensing and responding to cellular stress. Hence, the ER functions as a critical quality control organelle (Fu et al., 2021). During infection, the excessive production of viral proteins

burdens the protein folding machinery of the ER (Marques et al., 2024). This overload disrupts ER homeostasis, leading to the accumulation of misfolded or unfolded proteins, known as ER stress (Marques et al., 2024). The host cells have developed a response mechanism to prevent further buildup of unfolded proteins. The unfolded protein response (UPR) is the signaling system responsible for detecting the accumulation of unfolded or misfolded proteins and increasing the protein folding capacity to restore ER function (Chen et al., 2023; Read & Schröder, 2021). Mammalian cells have a complicated UPR that is mediated by three central ER transmembrane receptors: double-stranded RNA-activated protein kinase R (PKR)-like ER kinase (PERK), activating transcription factor 6 (ATF6), and type I transmembrane inositol-requiring enzyme 1 (IRE1α) (Chen et al., 2023; Read & Schröder, 2021). Each pathway has a distinct role in reducing ER stress and preserving cellular viability. By decreasing the transcription of secretory proteins and increasing the elimination of misfolded or slowly folding proteins by the pathways mentioned above, the UPR aims to prevent the accumulation of unfolded proteins (Read & Schröder, 2021).

PERK Pathway

One essential element of the unfolded protein response (UPR) triggered by ER stress is the protein kinase R-like ER kinase (PERK) pathway. Under normal conditions, PERK is kept inactive by the ER chaperone binding immunoglobulin protein (BiP), also called 78-kDa glucose-regulated protein (GRP78), which binds to the luminal domain of PERK. When misfolded or unfolded proteins accumulate in the ER and lead to ER stress, BiP preferentially binds to those misfolded proteins instead of PERK. This preferential binding of BiP to misfolded proteins allows PERK to dimerize (Bell et al., 2016). When

PERK dimerizes, it undergoes autophosphorylation, activating its kinase function. One of the primary targets of activated PERK is the eukaryotic initiation factor 2 alpha (eIF2α) (Bell et al., 2016). PERK phosphorylates eIF2α, leading to a significant decrease in protein synthesis. This results in less protein being produced and reduces the load on the ER machinery to manage the accumulated misfolded proteins. Lowering the number of new proteins entering the ER enables the ER machinery to operate more efficiently (Bell et al., 2016). Through these processes, the PERK pathway enhances the cell's stress tolerance and reduces protein influx into the ER (Bell et al., 2016). This complex response prepares the cell to endure prolonged stress while attempting to restore ER function (Bell et al., 2016; Read & Schröder, 2021).

ATF6 Pathway

Activating transcription factor 6 (ATF6) is initially localized in the ER membrane (Hillary & FitzGerald, 2018). During ER stress, when the ER becomes overloaded with misfolded proteins, ATF6 translocates from the ER to the Golgi apparatus (Horimoto et al., 2013). In the Golgi apparatus, ATF6 undergoes proteolytic cleavage by site-1 and site-2 proteases (S1P and S2P) (Hillary & FitzGerald, 2018; Horimoto et al., 2013). This cleavage releases the N-terminal cytosolic fragment of ATF6, which then migrates to the nucleus and acts as a transcription factor to start the transcription of UPR target genes (Hillary & FitzGerald, 2018; Horimoto et al., 2013). ATF6 induces the expression of chaperones, including binding immunoglobulin protein (BiP) and protein disulphide isomerase-associated 6 (PDIA6) (a member of the PDI family), all of which assist in refolding or degrading misfolded proteins, thereby alleviating ER stress (Hillary & FitzGerald, 2018).

In particular, Protein disulphide isomerase (PDI), a downstream transcriptional target of ATF6 signaling, plays a crucial role during ER stress (Hetz et al., 2020). It assists in protein folding by catalyzing the formation and rearrangement of disulphide bonds (Hetz et al., 2020). The upregulation of PDI reflects the cell's effort to enhance its folding capacity and alleviate ER stress (Hillary & FitzGerald, 2018; Hetz et al., 2020).

IRE1 Pathway

The unfolded protein response (UPR), which is triggered by a reaction to ER stress, also includes the inositol-requiring enzyme 1 (IRE1) pathway (Ishikawa et al., 2017). IRE1 undergoes oligomerization and autophosphorylation upon misfolded protein accumulation in the ER. IRE1 autophosphorylation initiates its endoribonuclease activity (Ishikawa et al., 2017) and forms IRE1α, which remains anchored in the ER membrane. The membrane localization of IRE1α facilitates efficient targeting and splicing of X-box binding protein 1 (XBP1) mRNA (Ishikawa et al., 2017). IRE1α removes a 26-nucleotide intron from XBP1 mRNA, resulting in a frameshift that produces the potent transcription factor XBP1s (Ishikawa et al., 2017). Like the ATF6 pathway, XBP1s translocates to the nucleus, stimulating the transcription of several UPR target genes, such as PDI (Ishikawa et al., 2017). ER-resident PDIs help form, break, and rearrange disulfide bonds in a range of proteins to support protein folding and proteostasis maintenance in the IRE1 pathway (Yuen et al., 2013). Furthermore, XBP1s stimulates lipid production, which is essential for expanding the ER membrane and meeting the increased requirements for protein folding during stressful conditions (Ishikawa et al., 2017).

Hence, in response to ER stress, the unfolded protein response (UPR) is activated to restore normal function by halting translation, upregulating chaperones, and increasing the degradation of misfolded proteins. However, persistent or unresolved ER stress shifts this protective response through the PERK, ATF6, and IRE1 pathways toward the activation of apoptosis through the activation of C/EBP Homologous Protein (CHOP), caspase-4, and caspase-12 (Szegezdi et al., 2006; Lee et al., 2010). These pathways often converge on the mitochondrial axis, where members of the Bcl-2 family play a crucial role in regulating apoptosis (Szegezdi et al., 2006).

Apoptosis and The Bcl-2 (B Cell Lymphoma-2) Family of Proteins

Apoptosis is a highly regulated process essential for maintaining cellular homeostasis by eliminating damaged or infected cells without triggering inflammation (Redza-Dutordoir & Averill-Bates, 2016; Elmore, 2007). It is one of many cellular mechanisms affected during viral infection and plays a critical role in influencing the outcome of viral replication (Marques et al., 2024). The primary organelles involved in controlling apoptosis are the mitochondria and the endoplasmic reticulum (ER) (Wu et al., 2023). Apoptosis is controlled by two main pathways: the extrinsic pathway, activated by external signals such as toxins and cytokines, and the intrinsic pathway, which originates within the cell due to stress caused by nutrient deficiency, prolonged accumulation of misfolded proteins, mitochondrial damage, oxidative stress or viral infection (Singh et al., 2019). The Bcl-2 (B-cell lymphoma 2) family of proteins play a vital role in regulating mitochondrial apoptosis, underscoring their key function in this process (Singh et al., 2019).

The Bcl-2 family as evolutionarily conserved regulators of apoptosis

The structures of Bcl-2 proteins have been highly conserved across nematodes to humans (Suraweera et al., 2022). The Bcl-2 family includes both pro-apoptotic and anti-apoptotic members, depending on whether they promote or inhibit apoptosis (Singh et al., 2019). The role of these proteins in the cell can be modified by cellular signaling, shifting the balance between survival and death (Qian et al., 2022). Therefore, an organism's ability to respond effectively to cellular stress relies on maintaining the proper balance between these proteins (Qian et al., 2022). It is also important to note that Bcl-2 family proteins operate between the endoplasmic reticulum (ER) and the mitochondria, regulating both the activation and inhibition of apoptosis (Singh et al., 2019).

Bcl-2 Subfamily group	Name of Protein	Structural domain
Anti-apoptotic proteins	Bcl-2	BH1, BH2, BH3, BH4
	Bcl-XL	BH1, BH2, BH3, BH4
	Mcl-1	BH1, BH2, BH3
Pro-apoptotic proteins	BAX	BH1, BH2, BH3
	BAK	BH1, BH2, BH3
	BOK	BH1, BH2, BH3
	Bcl-XS	BH3, BH4
BH3 domain only proteins	BAD	BH3
	BIM	BH3
	PUMA	BH3
	BID	BH3

Figure 1.1. A summary of the Bcl-2 family of proteins classified according to their subgroups and domains (Qian et al., 2022).

Bcl-2 homology (BH) domains and their contribution to the Bcl-2 family of proteins

Bcl-2 homology (BH) domains, including BH1, BH2, BH3, and BH4, are short conserved sequences of amino acids found in members of the Bcl-2 family (Qian et al., 2022; Warren et al., 2019). They are not separate proteins, but structural motifs that mediate protein-protein interactions and the regulation of apoptosis (Warren et al., 2019. These domains serve as the basis for classifying the Bcl-2 family into three subgroups: pro-apoptotic proteins, anti-apoptotic proteins, and pro-apoptotic BH3-only proteins (Qian et al., 2022). Anti-apoptotic proteins maintain mitochondrial integrity and prevent cell death by inhibiting apoptosis; they are homologous across all four domains - BH1, BH2, BH3, and BH4 (Brunelle & Letai, 2009). It is important to note that myeloid cell leukemia 1 (Mcl-1) lacks the canonical BH4 domain. Still, it retains BH1-BH3 domains that form the hydrophobic groove necessary to bind and inhibit pro-apoptotic proteins, allowing it to function as an anti-apoptotic protein. In contrast, pro-apoptotic proteins share sequence homology in the BH1, BH2, and BH3 domains but not in the BH4 domain (Brunelle & Letai, 2009). These proteins promote apoptosis by permeabilizing the outer mitochondrial membrane, leading to the release of cytochrome c and the activation of caspases, the enzymes responsible for executing cell death (Qian et al., 2022). Additionally, BH3-domain-only proteins support pro-apoptotic functions and share sequence homology exclusively with the BH3 domain (Kelekar & Thompson, 1998; Qian et al., 2022). Bcl-2 family proteins also feature a transmembrane domain at their C-terminus, which spans the cell's outer membrane and facilitates interactions with both the interior and exterior of the cell (Borgese et al., 2003). This transmembrane domain induces conformational changes that help localize and anchor Bcl-2 proteins to

the outer mitochondrial membrane, thereby regulating apoptosis (Borgese et al., 2003). Each BH domain can function independently or synergistically with other BH domains (Brunelle & Letai, 2009). A summary of the Bcl-2 family proteins, classified by subgroups and domains, is provided in Figure 1.1.

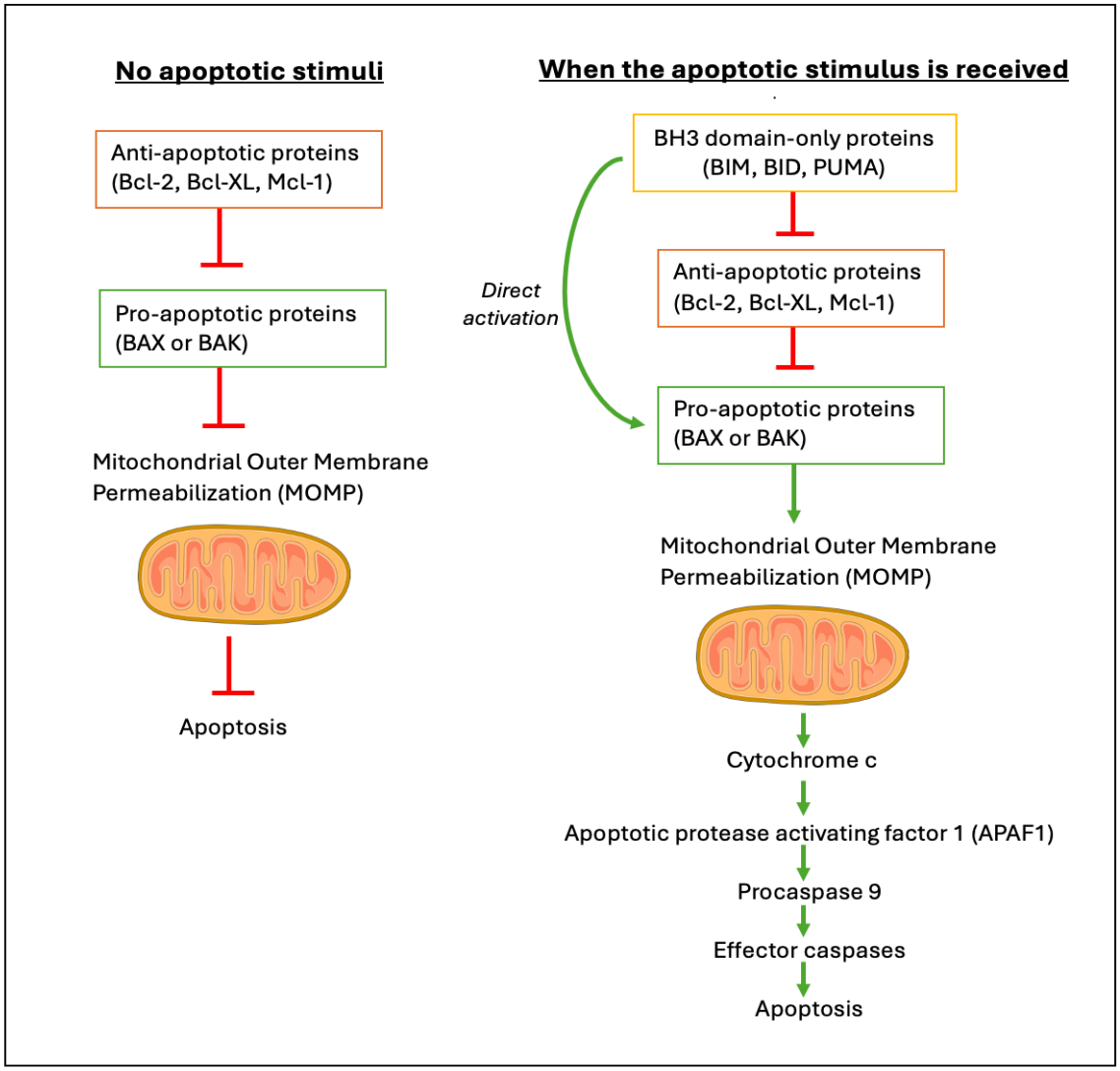

Figure 1.2. This figure shows a simplified flowchart illustrating the interaction between anti-apoptotic and pro-apoptotic members of the Bcl-2 family of proteins in the mitochondria (Aniogo et al., 2020; Brunelle & Letai, 2009; Prew et al., 2022).

Protein-protein interactions of Bcl-2 family members and their impact on Apoptosis

The regulation of apoptosis relies on interactions between pro-apoptotic and anti-apoptotic members of the Bcl-2 protein family (Brunelle & Letai, 2009; Prew et al., 2022). Typically, anti-apoptotic proteins, such as Mcl-1, prevent apoptosis by sequestering activated pro-apoptotic proteins, including BAX and BAK (Brunelle & Letai, 2009; Prew et al., 2022). This occurs through the formation of heterodimers, where the BH3 domain of BAX or BAK fits into a hydrophobic groove on the surface of Mcl-1, primarily formed by BH1-BH3 domains (Brunelle & Letai, 2009; Prew et al., 2022). This groove functions as a docking site, enabling Mcl-1 to bind tightly and neutralize pro-apoptotic proteins, thus preventing their oligomerization and insertion into the mitochondrial outer membrane (Brunelle & Letai, 2009; Prew et al., 2022). Consequently, mitochondrial integrity is maintained, cytochrome c release is inhibited, and the apoptotic process is halted, supporting cell survival under normal conditions (Brunelle & Letai, 2009; Prew et al., 2022) (Figure 1.2).

Adding to this regulatory network is prohibitin 1 (PHB1), a conserved protein primarily located in the inner mitochondrial membrane (Peng et al., 2015). Its anti-apoptotic function plays a crucial role in maintaining mitochondrial stability and preventing intrinsic apoptosis (Peng et al., 2015). PHB1 inhibits the activation of caspase-3 and supports the transcription and translation of anti-apoptotic genes, including Bcl-2 and Bcl-XL, thereby reducing mitochondrial outer membrane permeabilization and preventing the release of cytochrome c into the cytosol (Peng et al., 2015). This reinforces mitochondrial integrity and suppresses apoptotic signaling under non-stress conditions (Peng et al., 2015). Consequently, PHB1 contributes to mitochondrial

homeostasis by preserving mitochondrial morphology and dynamics, which are essential for proper mitochondrial function and overall cell survival.

However, when apoptotic signals are received, the balance shifts in favour of the pro-apoptotic proteins. The pro-apoptotic proteins, such as BAX and BAK, and the BH3-only proteins, like BID, promote apoptosis by forming pores on the mitochondrial outer membrane, which disrupts mitochondrial integrity and leads to mitochondrial membrane permeabilization (MOMP) (Brunelle & Letai, 2009; Prew et al., 2022). As a result of this permeabilization, apoptogenic factors, such as cytochrome c, are released into the cytosol from the mitochondrial intermembrane space (Prew et al., 2022). After entering the cytosol, cytochrome c forms the apoptosome complex by binding to apoptotic protease-activating factor 1 (APAF1) (Aniogo et al., 2020) (Figure 1.2). Subsequently, this complex activates procaspase-9, which in turn activates downstream effector caspases, such as caspase-3 and caspase-7. Caspase-3 and caspase-7 break down various proteins within the cell, including those involved in DNA repair and nuclear proteins, leading to distinctive morphological and biochemical features such as cell shrinkage, DNA fragmentation, membrane blebbing, and ultimately the formation of apoptotic bodies (Aniogo et al., 2020).

The BH3-only proteins provide additional regulation by acting as external sensors of cellular stress and delivering pro-apoptotic signals to the prominent pro-apoptotic and anti-apoptotic proteins (Prew et al., 2022). When BH3-only protein signaling outweighs the anti-apoptotic proteins, then latent monomers of BAX and BAK can be directly activated by specific BH3-only members, facilitating their oligomerization and the induction of MOMP (Brunelle & Letai, 2009; Prew et al., 2022). Altogether, the control

of apoptosis depends on the complex web of interactions between pro-apoptotic and anti-apoptotic Bcl-2 family members. The balance between anti-apoptotic proteins such as Bcl-2 and Mcl-1, and pro-apoptotic proteins like BAX and BAK, determines whether a stressed cell will survive or undergo apoptosis (Prew et al., 2022).

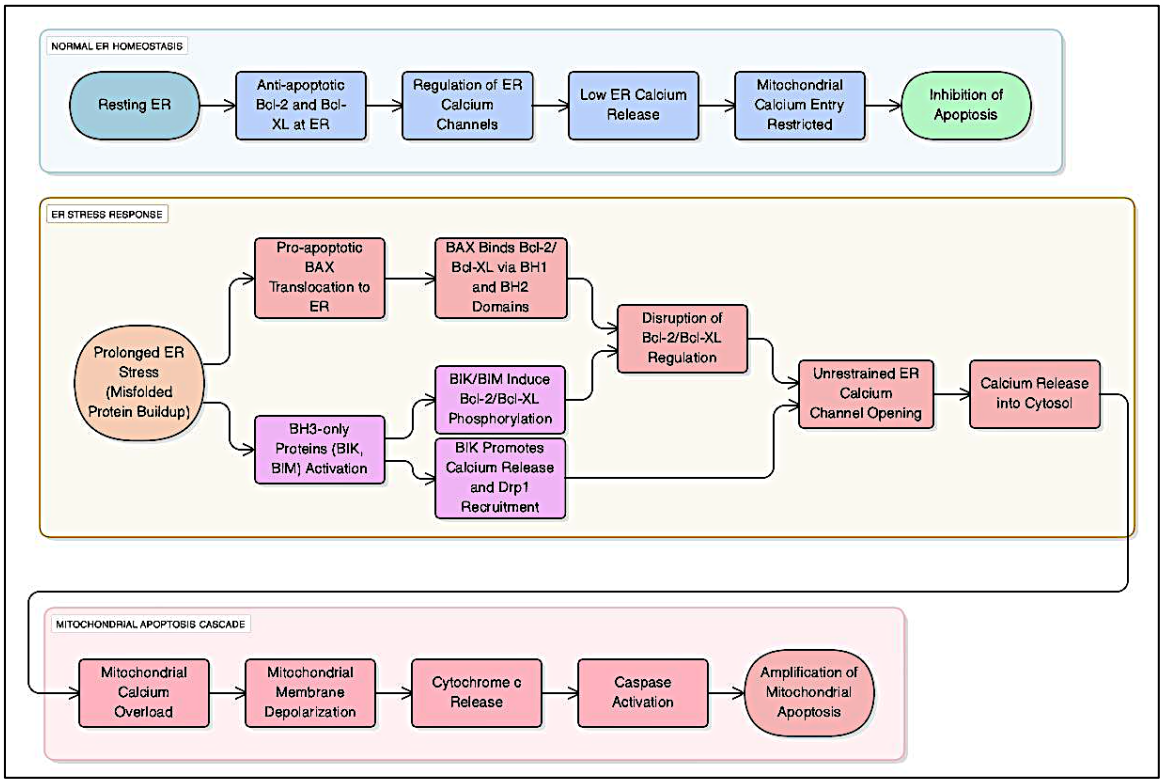

Figure 1.3. This figure shows a simplified diagram illustrating the interaction between anti-apoptotic and pro-apoptotic members of the Bcl-2 family of proteins at the endoplasmic reticulum (Jeong & Seol, 2008; Weston & Puthalakath, 2010).

Bcl-2 family members at the endoplasmic reticulum

Besides their well-known functions at the mitochondria, Bcl-2 family proteins also localize to the endoplasmic reticulum (ER), where they are essential for maintaining

calcium (Ca^{2+}) balance and regulating ER stress-induced apoptosis. Anti-apoptotic Bcl-2 family proteins such as Bcl-2 and Bcl-XL serve as key regulators of Ca^{2+} channels within the ER to prevent Ca^{2+} release into the cytosol. Overexpression of Bcl-2 has been shown to lower resting ER Ca^{2+} levels and restrict Ca^{2+} entry into mitochondria, thereby inhibiting Ca^{2}-dependent apoptotic signaling (Jeong & Seol, 2008; Weston & Puthalakath, 2010) (Figure 1.3).

However, during prolonged ER stress, such as from the buildup of misfolded proteins, the ER triggers apoptotic signals through Ca^{2}-dependent pathways (Jeong & Seol, 2008). A pro-apoptotic member of the Bcl-2 family, including BAX, translocates to the ER and binds to Bcl-2 family proteins via its BH1 and BH2 domains, disrupting their regulatory function. As a result, ER Ca^{2+} channels become unrestrained, releasing Ca^{2+} into the cytosol (Jeong & Seol, 2008; Szegezdi et al., 2009). This Ca^{2+} is then taken up by mitochondria, leading to mitochondrial Ca^{2+} overload, membrane depolarization, the release of cytochrome c, and activation of caspases, thereby amplifying mitochondrial apoptosis signaling (Jeong & Seol, 2008; Szegezdi et al., 2009) (Figure 1.3).

Additionally, BH3-only proteins such as BIK, which are anchored to the ER membrane, also play a crucial role in ER-mitochondria crosstalk during apoptosis (Jeong & Seol, 2008). During extended ER stress, BH3-only proteins like BIK and BIM become activated. These proteins induce phosphorylation of Bcl-2 and Bcl-XL, preventing them from regulating Ca^{2+} channels (Szegezdi et al., 2009; Boyce & Yuan, 2006) (Figure 1.3). BIK promotes Ca^{2+} release from the ER and recruits Drp1 (Dynamin-related protein 1) to the mitochondria, leading to cristae remodelling and mitochondrial outer membrane permeabilization, thereby enhancing the apoptotic process (Jeong & Seol, 2008).

These findings highlight the ER as an active site for apoptotic signaling and underscore the dual regulatory role of Bcl-2 family proteins in both ER and mitochondrial apoptosis pathways.

Viral Strategies to Modulate ER Stress and Apoptosis

Numerous viruses have developed complex mechanisms to either trigger or inhibit apoptosis(Cuconati & White, 2002; Takizawa et al., 1993). In many cases, viruses actively induce apoptosis to quickly eliminate host cells and promote viral spread. This strategy is particularly common among RNA viruses because of their rapid replication cycles (Cuconati & White, 2002; Koyama et al., 2000). For instance, the Influenza A virus replicates efficiently before the apoptotic process is complete and exploits host cell death to infect neighbouring cells (Ludwig et al., 2003; Takizawa et al., 1993).

In contrast, many double-stranded DNA viruses, including members of the *Herpesviridae* and *Poxviridae* families, encode specialized proteins that directly interfere with apoptotic signaling pathways and inhibit apoptosis (Cuconati & White, 2002). A notable example of this immune evasion strategy is the production of viral Bcl-2 homologs (vBcl-2). These viral proteins structurally and functionally mimic cellular Bcl-2 family members, thereby preventing apoptosis. They do so by inhibiting the pro-apoptotic activity of BH3-only proteins and preventing mitochondrial outer membrane permeabilization (Cuconati & White, 2002). For example, in the *Poxviridae* family, the fowlpox virus protein FPV039 encodes a vBcl-2 that closely resembles the host protein Mcl-1 (Banadyga et al., 2009). This viral protein binds to multiple BH3-only domain-containing proteins, thereby blocking apoptosis and supporting viral survival (Banadyga et al., 2009).

Although these strategies are well-established in several dsDNA viruses, little is known about how frog virus 3, which belongs to the *Iridoviridae* family, regulates endoplasmic reticulum (ER) stress responses and apoptotic pathways.

Frog virus 3: A Model Ranavirus of the *Iridoviridae* Family

Frog virus 3 (FV3) belongs to the genus *Ranavirus* within the family *Iridoviridae.* These are large, double-stranded DNA viruses that infect various ectothermic vertebrates, including amphibians, reptiles, and fish (Chinchar et al., 2011). FV3 was first isolated in the 1960s during attempts to culture Lucké herpesvirus in *Rana pipiens* (leopard frog) kidney cells (Granoff, 1966). Electron microscopy later revealed that FV3 has an icosahedral nucleocapsid, a characteristic feature of iridoviruses (Granoff, 1966). Because it was derived from frog kidney tissue, the virus was named "frog virus 3."

FV3 primarily targets the kidneys, leading to acute glomerular nephritis, which often proves lethal to infected hosts (Miller et al., 2007). The virus poses a severe threat to amphibian larvae and tadpoles because they are unable to clear the infection due to their developing immune systems (Daszak et al., 1999). Frog virus 3 has both necrotic and apoptotic effects. The necrotic and apoptotic effects of frog virus 3 in susceptible amphibians result in systemic, persistent cell death in numerous internal organs, which causes the host to die within a few days to several weeks after infection (Morrison et al., 2014). Frog virus 3 infection is also characterized by cutaneous symptoms such as skin ulceration, erythema, and body and limb edema. Bleeding in the kidneys and reproductive systems and pale, enlarged livers are also common symptoms (Morrison et al., 2014).

FV3 transmission occurs through contaminated water sources, direct contact with infected individuals, and parental transmission (Chinchar and Mao, 2011; Pearman et al., 2004). Additionally, FV3 can spread via avian vectors, contaminated fishing gear, and ranaculture systems (Schloegel et al., 2010). Although the connection between FV3 and global amphibian declines is still under investigation, FV3 has been linked to major die-offs worldwide (Carstairs et al., 2020). In Ontario, Canada, FV3 was identified in wild frog populations in 2004 and has since been associated with the death of up to 90% of certain amphibian populations across North America (Carstairs et al., 2020).

As mentioned above, FV3 infects a wide range of ectothermic vertebrates, including fish, amphibians, and reptiles. However, it is also capable of replicating in various cultured cell lines, including mammalian cells, provided the temperature is maintained between 12°C and 32°C (Granoff, 1966). Due to its broad host range and genomic features, FV3 serves as a valuable model for studying *Ranavirus* biology.

The FV3 genome comprises 105,903 base pairs and encodes 98 predicted open reading frames (ORFs) (Tan et al., 2004). This study focused on understanding the function of FV3 ORF 97R, which is the 97th open reading frame in the FV3 genome, with ‘R’ indicating it is transcribed from the rightward strand. FV3 97R encodes a putative vBcl-2 protein consisting of 137 amino acids (the 97R gene product) with an estimated molecular weight of approximately 15.3 kDa (Tan et al., 2004). The 97R gene is highly conserved within the *Ranavirus* genus (Tan et al., 2004; Ring et al., 2013). Comparative BLASTP analysis and Clustal Omega multiple sequence alignment reveal that many viral Bcl-2 homologs exhibit high sequence identity with FV3 ORF97R, indicating the conservation of functional motifs. The FV3 ORF97R (GenBank accession

no. AAT09757.1) exhibits 99% identity to STIV ORF103R (GenBank accession no. ACF42321.1), 99% to Chinese giant salamander iridovirus (CGSIV ORF101R) (GenBank accession no. AGV20632.1), 93% to TFV ORF104R (GenBank accession no. ABB92349.1), and 30.8% to SCRaV ORF41L (GenBank accession no. WHA35634.1). As 97R is a highly conserved gene, it is crucial to investigate its role in host-pathogen interactions and its contribution to the viral regulation of cellular processes, such as apoptosis.

Previous studies have shown that the FV3 97R localizes to the endoplasmic reticulum (ER) (Ring et al., 2013). Specifically, 97R was detected at the ER 24 hours post-transfection. It remains there through 48 hours, with increasing accumulation along the nuclear membrane and the appearance of ER invaginations into the nucleus at later time points (Ring et al., 2013).

Objective, Hypothesis and Prediction

Given the functional conservation observed among FV3 97R viral Bcl-2 homologs, its sequence identity to Mcl-1 (anti-apoptotic Bcl-2 family protein), its localization in the endoplasmic reticulum (ER), and its potential role in modulating host immune responses, characterizing the molecular interactions of FV3 97R with host binding partners is essential for understanding how FV3 influences host cell fate during infection. Although homologous proteins in related ranaviruses have been studied, the specific binding partners and cellular effects of FV3 97R remain unknown. Therefore, my research primarily aimed to investigate the functional role of the FV3 97R gene product while exploring its protein binding partners and the impact of FV3 97R on host cellular proteins, thereby improving our understanding of its function. I hypothesize that the FV3

97R gene product influences the host proteins involved in ER stress and mitochondrial apoptotic pathways. I predict that FV3 97R will interact with host proteins involved in these pathways, reflecting its role in modulating host cellular processes during infection. My research will help clarify the functional role of the FV3 97R gene product in regulating host cellular proteins. Insights gained from this study could inform future strategies to mitigate FV3 infections in ectothermic organisms, supporting conservation efforts for affected species.

CHAPTER 2

PREFACE

Title: **Frog virus 3 97R binds to cellular Prohibitin and decreases Protein Disulphide Isomerase levels**

Authors: **Lakshika Bansal**[1], **Samantha R Logan**[1], **and Craig R Brunetti**[1*]

[1]Department of Biology, Trent University, 1600 West Bank Drive, Peterborough, ON K9J 0G2, Canada.

[*]Address correspondence to the third author, craigbrunetti@trentu.ca

Contributions: The research presented in this thesis was conceived, supervised, and supported through funding secured by C.R.B. The overall study was carried out under the guidance and mentorship of C.R.B. Data analysis for the yeast two-hybrid screen was performed by S.R.L. All experiments and data analysis for the figures in this manuscript were carried out by L.B., who also captured and assembled all figures in this manuscript. L.B. prepared the first draft of the manuscript based on the findings.

Abstract

Frog virus 3 (FV3) belongs to the family *Iridoviridae* and the *Ranavirus* genus. FV3 encodes 97R, a putative viral Bcl-2-like (vBcl-2) protein that is similar in sequence to Mcl-1, the anti-apoptotic Bcl-2 family protein. However, the functional role of 97R in host-virus interactions remains uncharacterized. In this study, we investigated the effect of 97R on host cellular proteins. We transfected HeLa cells with 97R and performed indirect immunofluorescence assays that showed that 97R specifically reduces the expression of protein disulfide isomerase (PDI), an essential ER chaperone involved in protein folding and the unfolded protein response. This reduction occurred progressively over time, while levels of calnexin, another ER marker, remained unaffected. To identify potential host binding partners of 97R, we conducted a yeast two-hybrid screen using a truncated form of 97R. This screen identified prohibitin 1 (PHB1) as a high-confidence interactor. The interaction between 97R and PHB1 was then validated in mammalian cells through immunoprecipitation and western blot analysis. These findings provide functional evidence that FV3 97R selectively downregulates PDI and interacts with host proteins such as PHB1. Overall, this research reveals novel functions for FV3 97R, a vBcl-2-like protein, in interfering with ER proteins and highlights potential interactions that may be involved in immune regulation and FV3 pathogenesis.

Importance

Frog virus 3 infects amphibians, fish, and reptiles, leading to declines in their populations. Understanding how this virus interacts with host cells is crucial for uncovering how it causes infection. In this study, we examined a specific viral protein, 97R, which affects key functions within the host cell. We found that 97R decreases the level of a host protein involved in managing endoplasmic reticulum stress. We also discovered that 97R interacts with another host protein that helps regulate cell survival. These findings provide a new understanding of how frog virus 3 can disrupt normal cell functions to facilitate its replication.

Introduction

Ranaviruses are members of the *Iridoviridae* family, characterized by their large size and double-stranded DNA genomes [1]. They have been recognized as an emerging pathogen capable of infecting a wide range of ectothermic vertebrates, including amphibians, fish, and reptiles [1,2]. Their impact on both wild and cultivated populations has raised concern regarding their ecological and economic consequences [3]. The most well-characterized ranavirus is frog virus 3 (FV3). FV3 has served as a model system for studying virus-host interactions and understanding how viruses modulate host cellular processes to promote their replication [4]. While the general principles of FV3 replication are well established, the specific functions of many viral proteins remain undefined, hindering a complete understanding of how FV3 manipulates host cell processes [2]. Given their significant contribution to morbidity and mortality in ectotherms, such as amphibians, investigating individual FV3 genes is crucial for understanding the molecular mechanisms underlying their pathogenesis.

A key host cellular process commonly targeted by viruses to enhance replication and persistence is apoptosis [5,6]. Apoptosis, a highly regulated biochemical process, can lead to programmed cell death in response to internal and external stressors, including viruses [6]. Numerous viruses have developed mechanisms to inhibit, delay, or even induce apoptosis, thus increasing their replication while evading host immune responses [5, 6, 7]. Apoptosis is primarily regulated by members of the B-cell lymphoma (Bcl-2) protein family, which act as essential molecular checkpoints that integrate ER stress signals and determine the cellular decision to undergo programmed cell death [8]. The Bcl-2 family of proteins exhibits both pro-apoptotic and anti-apoptotic functions through

dynamic interactions at the mitochondrial and endoplasmic reticulum (ER) membranes [8]. Bcl-2 family proteins are characterized by conserved Bcl-2 homology (BH) domains, BH1, BH2, BH3, and BH4, which support their structure and function [8]. Bcl-2 proteins also contain a C-terminal transmembrane domain that anchors them to intracellular membranes, including those of the mitochondria and endoplasmic reticulum [9, 10, 11]. The composition and arrangement of BH domains determine whether a protein promotes or inhibits apoptosis. Proteins containing BH1 to BH3 generally promote cell death, while those incorporating all four domains, particularly BH1 and BH2, act as inhibitors of apoptosis [12, 13].

Several ranaviruses encode viral Bcl-2-like proteins (vBcl-2), which play a crucial role in modulating apoptosis. For example, the tiger frog virus (TFV) ORF104R has been extensively studied. It is localized to mitochondria and encodes a 149-amino acid vBcl-2 protein that contains a BH1 domain and a C-terminal transmembrane domain, which are characteristic features of Bcl-2 family proteins [14]. This protein interacts with voltage-dependent anion channel 2 (VDAC2), a mitochondrial membrane protein, and inhibits apoptosis in NIH3T3 cells, suggesting a role in suppressing host cell death during infection [14]. Additionally, grouper iridovirus (GIV) ORF66R, which is localized to the outer mitochondrial membrane, contains a BH3 domain and a C-terminal transmembrane domain. These features are crucial for its role in inhibiting apoptosis by sequestering Bim, a pro-apoptotic member of the Bcl-2 family [15].

The FV3 genome consists of 105,903 base pairs and encodes 98 predicted open reading frames (ORFs) [4]. FV3 also encodes a putative vBcl-2 protein, 97R, that has 93% sequence identity to TFV ORF104R (Figure 2.1A) [14, 16]. The 97R gene product

consists of 137 amino acids, with a predicted molecular weight of approximately 15.3 kDa [2, 4, 9]. BLASTP alignment shows that the 97R gene product exhibits 33% sequence identity over a 36-amino-acid region with myeloid cell leukemia-1 (Mcl-1) from *Xenopus laevis* (Figure 2.1B) [16]. More specifically, the 97R gene product features identifiable BH1 and BH2 domains, with the BH1 domain being relatively well conserved and aligning notably with the BH1 domain of Mcl-1 (Figure 2.1B & C) [17]. Mcl-1 is an anti-apoptotic member of the Bcl-2 family known for inhibiting apoptosis by anchoring to the mitochondria and endoplasmic reticulum to promote cell survival [18]. Furthermore, the C-terminal portion of 97R exhibits a hydrophobic stretch resembling a transmembrane domain, which corresponds with the membrane association profile of canonical anti-apoptotic Bcl-2 proteins (Figure 2.1B & C) [9, 19, 20]. Previous studies have demonstrated that the FV3 97R localizes to the endoplasmic reticulum (ER) [9]; 97R was observed at the ER at 24 hours post-transfection and remained localized there through 48 hours, with progressive accumulation along the nuclear membrane and the appearance of ER invaginations into the nucleus at later time points [9]. The ER localization was shown to depend on the C-terminal region of the protein. Deleting the final 29 amino acids corresponding to the transmembrane domain of 97R abolished ER targeting [9]. These findings support the predicted presence of a C-terminal transmembrane domain, suggesting that the ER is a likely site of action for the FV3 97R gene product.

Interestingly, TFV 104R and FV3 97R have different subcellular localizations despite their high sequence identity; TFV 104R localizes to the mitochondria [14], while FV3 97R primarily localizes to the endoplasmic reticulum [9]. This difference may result

from virus-specific modifications in the C-terminal transmembrane region (Figure 2.1A) [14], which can alter protein interactions with the host cell machinery. The precise roles of the 97R and its host-binding partners remain unknown; similarity to TFV 104R and GIV 66R may suggest a conserved function in modifying host cell survival pathways at different subcellular sites through ER-mitochondria crosstalk.

Given the functional conservation observed among FV3 97R homologs, its localization in the endoplasmic reticulum (ER), and its potential role in modulating host immune responses, characterizing the molecular interactions of FV3 97R with host binding partners is crucial for understanding how FV3 influences the fate of host cells. While homologous proteins in related ranaviruses have been studied, the specific binding partners and cellular effects of FV3 97R remain unclear. This study examined the functional role of the 97R gene product. We investigated the protein binding partners and the impact of FV3 97R on host cellular proteins to enhance our understanding of 97R function.

Methods

Cell lines and Antibodies

HeLa (Henrietta Lacks) cells were obtained from the American Type Culture Collection (ATCC, Manassas, VA). They were cultured in Dulbecco's Modified Eagle's Medium (DMEM; ThermoFisher Scientific, Massachusetts, USA), supplemented with 10% fetal bovine serum (FBS; ThermoFisher Scientific, Massachusetts, USA), 1% (v/v) amphotericin B, and 1% (v/v) penicillin/streptomycin, and maintained at 37°C with 5% CO_2.

The following antibodies were used for immunofluorescence experiments: rabbit anti-Myc (1:400; Fitzgerald Industries International, MA), mouse anti-protein disulfide isomerase (PDI; 1:75; Thermo Fisher Scientific, Canada), mouse anti-calnexin (1:100; Thermo Fisher Scientific, Canada), FITC-conjugated goat anti-rabbit IgG (1:100; Jackson ImmunoResearch Laboratories Inc., West Grove, PA), Cy5-conjugated goat anti-mouse IgG (1:100; Jackson ImmunoResearch Laboratories Inc.). For Western Blot, we used mouse anti-Myc (Abcam, catalog no. ab18185), rabbit anti-prohibitin (Abcam, catalog no. ab75766), mouse anti-PDI (Thermo Fisher Scientific, catalog no. MA3-019), rabbit anti-Myc (Abcam, catalog no. ab314108), rabbit anti-prohibitin (1:10,000; Abcam, catalog no. ab75766), mouse anti-Myc (1:1,000; Abcam, catalog no. ab18185), mouse anti-PDI (1:1,000; Thermo Fisher Scientific, catalog no. MA3-019), and rabbit anti-Myc (1:300; Abcam, catalog no. ab314108).

Codon Optimization and Cloning

FV3 97R was codon-optimized by GenScript (Piscataway, NJ) and cloned using the pTARGET Mammalian Expression Vector System (Promega, Madison, WI) according to the manufacturer's protocol (Co97R pTARGET) (Ring et al., 2013).

Plasmid DNA extraction

Bacterial colonies were grown in 5 mL glass Erlenmeyer flasks containing 5 mL of Luria Bertani (LB) Broth (500 mL diH_2O, 5 g Bacto tryptone, 2.5 g Bacto yeast extract, and 5 g NaCl) and 5 µL of 20 µg/mL ampicillin (Sigma-Aldrich, Oakville, ON), shaking at 250 RPM at 37°C for 12 hours. The 5 mL cultures were then transferred to 250 mL glass Erlenmeyer flasks containing 50 mL of LB Broth with 50 µL of 20 µg/mL

ampicillin and shaken at 250 RPM at 37°C for 16 hours. To extract the plasmid, the QIAGEN Plasmid Midi kit (QIAGEN, Toronto, Canada) was used according to the manufacturer's instructions. The concentration of the extracted plasmid was measured using the BioTek Synergy HTX Multimode Reader (Agilent Technologies, Santa Clara, California, USA).

Transfection

HeLa cells were grown on 6-well plates (Progene, Ultident Scientific) with coverslips to 75% confluency. 10 µL of Lipofectamine 2000 transfection reagent (Life Technologies, Burlington, ON) was used to transfect HeLa cells with 4 µg of Myc-Co97R pTarget plasmid. Transfection complexes were added to the cells in 6-well plates, along with 2 mL of 10% FBS-supplemented DMEM, and incubated for 12, 18, 24, 36, and 48 hours at 37°C and 5% CO_2. For the plates incubated for 36 and 48 hours, the culture medium was replaced with fresh 10% FBS-supplemented DMEM at 24 hours to maintain cell viability. To transfect the T75 cm^2 culture flasks, HeLa cells were also grown to 75% confluency in the culture flasks. Cells were transfected according to the manufacturer's instructions (Life Technologies, Burlington, ON). Briefly,100 µL of Lipofectamine 2000 transfection reagent was used to transfect HeLa cells with 40 µg of the Myc-Co97R pTarget plasmid. Transfection complexes were added to the cells in T75 cm^2 flasks, along with 15 mL of 10% FBS-supplemented DMEM and incubated for 24 hours at 37°C and 5% CO_2. For mock-transfected cells (used as a control), the transfection complexes contained only Lipofectamine 2000 (10 µL for 6-well plates and 100 µL for T75 cm^2 flasks). Following transfection, the medium was replaced with 2 mL and 15 mL of 10% FBS-supplemented DMEM, respectively.

Indirect immunofluorescence

HeLa cells were cultured to 75% confluency on a coverslip in a 6-well plate. The cells were washed twice with 1X phosphate-buffered saline (PBS) (pH 7.4, ThermoFisher Scientific, catalog number 10010023) and fixed with 1 mL of 3.7% paraformaldehyde (0.444g paraformaldehyde, 12 mL PBS and 3 µL of 10N NaOH) for 10 minutes. The cells were washed twice with 1X PBS for 2 minutes and permeabilized with 1 mL of 0.1M Triton X-100 for 5 minutes. Cells were washed twice with 1X PBS, followed by 2 mL of blocking buffer (5% Bovine Serum Albumin (BSA; Sigma-Aldrich), 50 mM Tris-HCl (pH 7.4), 150 mM NaCl, 0.5% NP-40), and incubated at room temperature for 2 hours. The cells were washed twice for 3 minutes with wash buffer (1% BSA, 50 mM Tris-HCl (pH 7.4), 150 mM NaCl, 0.5% NP-40). Primary antibodies (100 µL) diluted in blocking buffer were incubated for 1 hour. The cells were washed twice with wash buffer for 3 minutes. Following this, 100 µL of the secondary antibodies, were added to the coverslip and incubated for 1 hour at room temperature. After removing the antibodies, the cells were washed twice with the wash buffer for 3 minutes. Coverslips were mounted on slides using VECTASHIELD (4', 6-diamidino-2-phenylindole; Vector Laboratories, Burlington, ON, Canada) and sealed with clear nail polish (Sally Hansen Insta-Dri). The Leica DM IRE2 fluorescent microscope (Leica, Concord, ON, Canada) was used to detect fluorescence.

Yeast Two-Hybrid Screen

A yeast two-hybrid (Y2H) screen was conducted by Hybrigenics Services (Paris, France) to identify potential protein interactors of the FV3 97R. The coding sequence corresponding to amino acids 1–112 of the FV3 97R gene product (Fig. 1C) was cloned

into the pB43 vector as an N-terminal fusion to the GAL4 DNA-binding domain for use as bait. This bait was screened against a *Xenopus laevis* embryo cDNA library fused to the GAL4 activation domain (prey) using the ULTImate Y2H platform. Corresponding interacting proteins were identified through an automated procedure via GenBank (NCBI), and each interaction was assigned a Predicted Biological Score (PBS) ranging from A (high confidence) to F (low confidence).

Immunoprecipitation

HeLa cells were grown to 90% confluency in a T75 cm^2 flask. The media was removed, and 5 mL of PBS (pH 7.2) (ThermoFisher Scientific) was added. Using a sterile scraper, all cells were detached from the T75 cm^2 flask, and the resulting solution was transferred to a 15 mL Falcon tube. The cell suspension was centrifuged at 3000 x g for 6.5 minutes at room temperature. The supernatant was discarded, and the pellet was resuspended in 1 mL of Pierce IP Lysis Buffer (0.025M Tris, 0.15M NaCl, 0.001M EDTA, 1% NP-40, 5% glycerol, pH 7.4; ThermoFisher Scientific, ON). The resuspended lysate was then transferred to a microcentrifuge tube and incubated on ice for 5 minutes. After 5 minutes, the solution was centrifuged at 13000 x g for 10 minutes at 4°C. The concentration of the lysate was determined using the Qubit Protein Assay Kit (ThermoFisher Scientific; catalog number Q33211). Lysate was immunoprecipitated using the Pierce Classic IP Kit (ThermoFisher Scientific, ON; Catalog no. 26146). Whole-cell lysate was pre-cleared with 1 mg of lysate with 80 µL of Pierce control agarose resin slurry in a Pierce Spin Column placed in a microcentrifuge tube. The resin was first washed with 100 µL of 0.1 M sodium phosphate (pH 7.2) and 0.15 M sodium chloride (pH 7.2), followed by centrifugation at 1000 × g for 1 minute. After discarding

the flow-through, 1 mg of whole-cell lysate was added to the resin and incubated at 4 °C for 1 hour with end-over-end mixing. After 1 hour, the column was centrifuged, and the flow-through, containing the pre-cleared lysate, was collected in a microcentrifuge tube and kept on ice. For immune complex formation, 3 µL of antibody was added to the pre-cleared lysate, adjusting the final volume to 500 µL with Pierce IP Lysis Buffer. This mixture was incubated at 4°C for 1 hour. To capture the immune complexes, 20 µL of Pierce protein A/G agarose slurry was added to a new Pierce spin column. The resin was washed twice with 100 µL of cold IP Lysis Buffer and centrifuged after each wash. Excess liquid was removed by tapping the column. The antibody-lysate mixture was added directly to the column, and the sample was incubated at 4°C for 1 hour with end-to-end mixing to allow binding to the resin. After incubation, the column was centrifuged to collect unbound flow-through. The resin was washed once with 200 µL IP Lysis Buffer, followed by three additional washes with the same buffer to ensure the removal of non-specifically bound proteins. A final rinse with 100 µL of 1X Pierce IP Conditioning Buffer (neutral pH buffer provided in the Pierce Classic IP kit by ThermoFisher Scientific) was performed to prepare for elution. Elution was done by adding 50 µL of 2X non-reducing Lane Marker Sample Buffer (0.3M Tris HCl, 5% SDS, 50% glycerol, lane marker tracking dye; pH 6.8) and 20 mM Dithiothreitol (DTT) directly to the resin. The column was incubated at 100°C for 10 minutes and centrifuged to collect the eluate. Samples were cooled to room temperature and used for SDS-PAGE and Western blot analysis.

SDS-PAGE and Western Blotting

Protein samples (30 µg per lane) were resolved by SDS-PAGE on 10–20% Novex Tris-Glycine gels (ThermoFisher Scientific, MA, USA) at a constant voltage of 125 V for 1 hour and 40 minutes. Proteins were transferred to 0.2 µm nitrocellulose membranes (ThermoFisher Scientific, MA, USA) using a wet transfer system at 10 V for 1 hour. Following the protein transfer, membranes were washed three times for 5 minutes with 1X TBST (20 mM Tris-HCl, pH 7.6; 150 mM NaCl; 0.1% Tween-20) and then blocked on a shaking platform for 1 hour at room temperature in 1X TBST supplemented with 5% (w/v) non-fat dry milk. Membranes were incubated with the primary antibodies diluted in the blocking buffer for 1 hour at room temperature on a shaking platform. After blocking, membranes were washed in 1X TBST three times for 5 minutes and probed with HRP-conjugated Clean-Blot IP Detection Reagent (1:1000, ThermoFisher Scientific) for 1 hour. Membranes were washed thrice for 5 minutes in 1X TBST. Proteins were visualized using Clarity Western ECL substrate (Bio-Rad Laboratories, CA, USA) and imaged using the ChemiDoc MP Imaging System (Bio-Rad Laboratories).

Data Analysis

Immunofluorescence intensity of PDI was quantified using ImageJ. Multi-channel images were first split into individual channels, and the PDI-specific channel was isolated for fluorescence analysis. For each image, individual cells were outlined manually using the freehand selection tool to define the region of interest (ROI). The “Measure” function of ImageJ was then used to obtain the integrated density, mean gray value, and cell area. To correct for background fluorescence, an ROI of the same size was drawn in a region lacking cells within the same field of view, and its mean gray value was recorded. Corrected total cell fluorescence (CTCF) was calculated using the formula: CTCF for

PDI = Integrated Density – (Area of selected cell x Mean fluorescence of background readings). For quantification, 40 cells showing Myc-97R staining (transfected cells) were specifically selected for measurement of PDI fluorescence intensity at each time point (12, 18, 25, 36, and 48 hours). For the 0-hour time point, when no Myc-97R staining was present, 40 random cells were chosen to establish baseline PDI fluorescence. Data from each biological replicate (40 cells per time point) were averaged to obtain a mean CTCF value, and the means from three independent experiments (n = 3) were used for statistical analysis.

Quantitative data, including fluorescence intensity measurements from immunofluorescence images, were analyzed using GraphPad Prism (Version 10.4.2 (534); GraphPad Software, San Diego, CA). Statistical comparisons of mean CTCF at various times post-transfection were performed using one-way analysis of variance (ANOVA), followed by Tukey's multiple comparisons post-hoc test to identify significant differences between PDI and calnexin intensity at different times post-transfection. A p-value < 0.05 was considered statistically significant.

Results

97R expression does not affect calnexin levels but reduces PDI expression in a time-dependent manner

Studies have demonstrated that FV3 97R localizes to the endoplasmic reticulum (ER) [9], indicating it may influence ER function. To determine whether 97R expression affects the levels of specific ER markers, we measured two well-characterized ER proteins: protein disulfide isomerase (PDI) and calnexin. PDI is a soluble ER-resident

enzyme that facilitates disulfide bond formation [21], while calnexin is an integral ER membrane protein involved in glycoprotein folding [22]. HeLa cells were transfected with 97R, and immunofluorescence staining for PDI and calnexin was observed at 0, 12, 18, 24, 36, and 48 hours post-transfection. The 0-hour time point represents non-transfected cells.

In cells expressing 97R, we observed a gradual decline in PDI levels over time (Figure 2.2A & B), whereas no such decline was seen in cells not expressing 97R at the same time points (Figure 2.2C). Immunofluorescence staining showed that PDI intensity was similar at early time points (0, 12, and 18 hours post-transfection), but a decline became evident by 24 hours, becoming more noticeable at 36 and 48 hours (Figure 2.2A). Statistical analysis revealed no significant differences between 0 and 12 hours ($p > 0.9999$) or between 12 and 18 hours ($p = 0.9998$), indicating that 97R expression does not influence PDI levels during early stages of transfection (Figure 2.2B). However, significant decreases in PDI fluorescence were observed at 24 hours ($p = 0.0200$), 36 hours ($p = 0.0012$), and 48 hours ($p = 0.0036$) compared to 12 hours. Additional comparisons between 18 hours and both 36 and 48 hours also showed significant differences ($p = 0.0021$ and $p = 0.0007$, respectively), supporting a time-dependent decline in PDI expression in response to 97R (Figure 2.2B).

In contrast, immunofluorescence analysis revealed no significant changes in calnexin expression in the HeLa cells expressing 97R at any of the time points post-transfection (Figure 2.3A & B). Similarly, calnexin levels in HeLa cells that did not express 97R remained stable across the same time points (Figure 2.3C), with no significant differences observed ($p \geq 0.5$). These results show that 97R specifically causes

PDI downregulation in the HeLa cells expressing 97R, indicating that 97R does not lead to general disruption or downregulation of all ER-resident proteins. Instead, the effect of 97R is very specific to PDI.

Yeast Two-Hybrid (Y2H) screen identified prohibitin (PHB1) as a potential binding partner of FV3 97R

Given the observed reduction in PDI expression, we sought to identify host proteins that may interact with 97R. Although TFV 104R was shown to bind VDAC2 [14], which is a mitochondrial protein, 97R may interact with a different subset of proteins. To identify the binding partners of FV3 97R, a yeast two-hybrid (Y2H) screen was performed using a truncated form of 97R (aa 1-112), which lacks the C-terminal transmembrane domain (Fig. 1C), as bait against a cDNA library from *Xenopus laevis* embryos. Before the screening, it was confirmed that 97R was non-toxic but exhibited autoactivation activity. The screen assessed over 105 million interactions and produced 344 positive clones. These clones were classified using the Hybrigenics PBS scoring system (data not shown). These initial results provided several candidate interactors for further validation of 97R-host protein interactions. Although PDI or VDAC2 were not among the identified interactors, prohibitin 1 (PHB1), an anti-apoptotic protein localized to the inner mitochondrial membrane, emerged as a high-confidence binding partner for 97R.

FV3 97R binds to prohibitin (PHB1) in HeLa Cells

Since prohibitin 1 (PHB1) was identified as a high-confidence 97R interactor in the yeast two-hybrid screen, we performed immunoprecipitation and Western blot assays in HeLa cells to validate this interaction. HeLa cells transfected with Myc-tagged 97R were lysed after 24 hours, and Myc-tagged 97R was immunoprecipitated with an anti-Myc antibody. The precipitates were analyzed by Western blot using an anti-PHB1 antibody to assess co-precipitation. Our results showed that PHB1 (~30 kDa) was detected in the Western blot in the 97R-transfected lane, but not in the control, mock-transfected lane (Figure 2.4A & B). These data support an interaction between 97R and PHB1, which was originally identified in our yeast two-hybrid (Y2H) screen.

To further validate the interaction, we carried out a reverse IP for PHB1 and Western blotted for Myc-tagged 97R. FV3 97R (~17 kDa) was detected in lysates from 97R-transfected cells but not in cells that were mock-transfected (Figure 2.5). These immunoprecipitation results validate the Y2H screen findings and support a physical interaction between 97R and PHB1 in mammalian cells.

Discussion

This study aimed to understand how the viral protein FV3 97R affects host cells and interacts with host proteins. Previous research has shown that 97R localizes to the endoplasmic reticulum (ER), suggesting it may influence ER proteins. To explore this, we examined whether 97R alters the levels of ER-localized proteins and investigated the host proteins with which it interacts. Both PDI and calnexin are ER-resident proteins involved in protein quality control [21, 22]. The absence of any observable change in calnexin suggests that the reduction in PDI is not part of a general degradation of ER proteins but instead points to a more selective effect.

The selective downregulation of protein disulfide isomerase (PDI), but not calnexin, in HeLa cells expressing 97R suggests that FV3 97R causes a specific disruption of ER function rather than a general suppression of ER-resident proteins. PDI is a multifunctional 57 kDa chaperone that plays a key role in protein folding by catalyzing the formation and rearrangement of disulfide bonds between cysteine residues in proteins in the ER [23, 24]. Besides its role in protein folding, PDI is also involved in regulating the ER stress response [25]. PDI is a downstream target of the Activating Transcription Factor 6 (ATF6) pathway in the unfolded protein response (UPR), which is activated during ER stress (Hetz et al., 2020). UPR is a protective mechanism that restores protein-folding capacity and maintains cellular homeostasis [25]. During the ATF6 pathway of UPR, PDI is usually upregulated to increase the ER's folding capacity and ensure protein quality control [25]. It facilitates the formation and rearrangement of disulfide bonds, a vital process for the maturation of secretory and membrane proteins [25]. Therefore, the suppression of PDI in 97R-expressing cells may indicate a disruption of this adaptive ER stress response. This disruption could compromise proper protein folding in the ER, leading to the further accumulation of misfolded proteins and ultimately disrupting cellular homeostasis in a way that may favour viral replication.

Although we did not directly measure viral replication in our study, previous reports indicate that several viruses, including human immunodeficiency virus (HIV) and human cytomegalovirus (CMV), target PDI to support their life cycle or evade immune detection. In HIV, the envelope glycoprotein gp120 interacts with PDI, which catalyzes the reduction of disulfide bonds within gp120 [26]. This reduction is a crucial step that enables gp120 to undergo the necessary conformational changes for binding to the CD4

receptor and initiating membrane fusion during viral entry. In contrast, CMV (Herpesvirus-5) employs a different strategy through its US3 protein, which degrades PDI, thereby impairing the antigen-presenting function of MHC class I molecules [27]. This allows the virus to avoid recognition and clearance by cytotoxic T lymphocytes [27, 28]. Whether FV3 takes advantage of a comparable mechanism remains to be established, but our findings suggest a potential for further investigation.

Although PDI levels are noticeably reduced following 97R expression, our current data do not establish a direct interaction between the two proteins. PDI was not identified in our yeast two-hybrid (Y2H) screen. Therefore, while the correlation between 97R expression and PDI downregulation is significant, this phenotype might occur indirectly, possibly through broader disruption of ER homeostasis or stress pathways. Future experiments should aim to measure PDI mRNA levels, perform proteasomal degradation assays, or utilize reporter assays to investigate the unfolded protein response. These approaches will help determine whether PDI downregulation occurs at the transcriptional or post-transcriptional level, or due to proteostasis imbalance caused by FV3 97R.

In contrast to PDI, our yeast two-hybrid (Y2H) screen identified prohibitin 1 (PHB1) as a potential interacting partner of 97R. PHB1 is a highly conserved protein expressed in a wide range of cell types and is predominantly localized to the mitochondria, although it is also found in the nucleus and plasma membrane [29]. It has a molecular weight of 30 kDa and contains a transmembrane domain [29, 30]. Depending on its subcellular localization, PHB1 is involved in diverse cellular processes, including the regulation of cell proliferation, transcription, and apoptosis [29]. Notably, PHB1 has

been shown to play a protective role against apoptosis, with knockdown increasing susceptibility to apoptotic stimuli and overexpression promoting resistance [29]. In granulosa cells, PHB1 overexpression has been linked to upregulation of anti-apoptotic Bcl-2 family proteins such as Mcl-1, further highlighting its role in apoptosis suppression [31]. In our study, immunoprecipitation followed by western blot analysis confirmed an interaction between FV3 97R and PHB1 in transfected HeLa cells. As the endoplasmic reticulum (ER) membrane is continuous with the nuclear membrane, it is plausible that PHB1 and 97R are positioned in close proximity within the cell, potentially enabling biological interaction. However, since immunoprecipitation assays were conducted on lysed cells, disruption of intracellular compartments during lysis may allow proteins to interact *in vitro*. Therefore, while our data demonstrate that 97R and PHB1 interact under experimental conditions, further research is needed to establish a functional interaction between FV3 97R and PHB1 during FV3 infection. Future studies could employ techniques such as proximity ligation assays to determine whether 97R and PHB1 interact functionally during FV3 infection, providing in situ evidence within the context of viral replication.

Furthermore, the biological significance of the 97R-PHB1 interaction remains to be elucidated. Since PHB1 has been linked to various cellular processes, including the regulation of apoptosis, mitochondrial dynamics, and cell cycle control [29], it is still uncertain whether its interaction with 97R has functional consequences on any of these pathways during FV3 infection.

Our findings contribute to a growing understanding of how ranaviruses disrupt host cellular mechanisms and may highlight potential differences in host manipulation

strategies among viral species. Previous studies have demonstrated that TFV 104R interacts with the mitochondrial protein voltage-dependent anion channel 2 (VDAC2), a key regulator of mitochondrial membrane permeability and apoptosis [14]. This interaction suggests that TFV 104R directly influences mitochondrial apoptotic pathways. In contrast, our study indicates that FV3 97R may also affect host cell processes. We identified PHB1, a multifunctional protein involved in apoptosis regulation, as a binding partner for 97R, and observed that 97R expression causes a selective reduction in the ER-resident chaperone PDI. Although TFV 104R and FV3 97R share significant sequence identity and conserved structural domains, they are present in different organelles, perhaps mediated by significant differences in the transmembrane domains (Figure 2.1A). Our results suggest that their host binding partners, and cellular targets differ. This divergence may reflect evolutionary adaptations that enable different ranaviruses to exploit distinct host environments.

Finally, we utilized human HeLa cells as a model system to investigate the molecular interactions of FV3 97R. HeLa cells are commonly used in cell biology research due to their well-characterized biology, ease of handling and genetic manipulation, and the wide availability of molecular tools and reagents. However, FV3 is a natural pathogen of ectothermic vertebrates such as amphibians, and it remains unclear whether these interactions or changes in protein expression observed in this study occur in the natural host. Notably, the yeast two-hybrid screen that identified PHB1 as a 97R-interacting protein was performed using *Xenopus* cDNA library, indicating that this interaction is conserved between human and *Xenopus* PHB1 and thus biologically relevant even when observed in HeLa cells. Nonetheless, previous studies on TFV 104R

were also conducted using mammalian systems, where TFV 104R was shown to inhibit apoptosis in NIH3T3 cells [14], supporting the use of mammalian cells as a valid platform for initial functional characterization. Future studies would benefit from extending these observations to amphibian or fish cell lines, ideally under conditions of natural FV3 infection, to assess the conservation and biological relevance of the findings reported here.

In conclusion, this study suggests a potential functional role for FV3 97R, a viral protein localized to the endoplasmic reticulum (ER). We demonstrate that 97R expression selectively reduces PDI levels over time without affecting calnexin, indicating a targeted impact on ER protein homeostasis. The decrease in PDI expression prompts questions about whether 97R influences ER stress. Additionally, we identify PHB1 as a host binding partner of FV3 97R through yeast two-hybrid screening, immunoprecipitation, and western blot analysis in HeLa cells. While these findings imply that 97R may interact with multiple host cellular pathways, further research is required to establish the functional significance of these interactions. Our use of HeLa cells offers a suitable system for initial characterization, although validation in amphibian cells during FV3 infection will be essential to fully understand the functional role of 97R in host cell modulation.

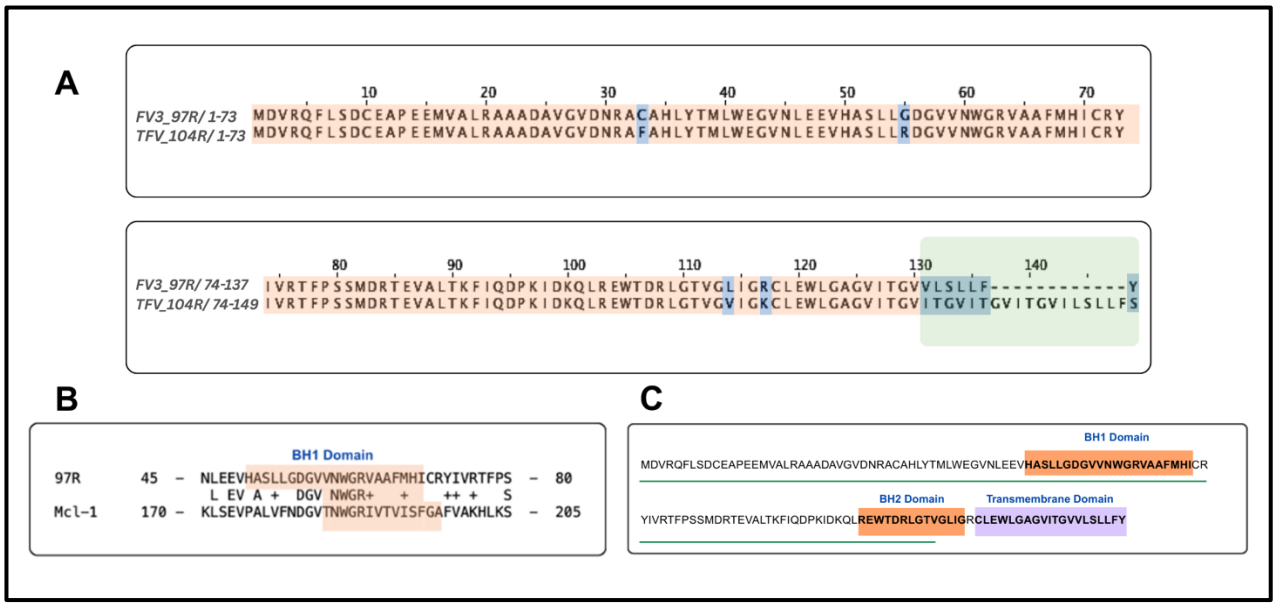

Figure 2.1. (A) Multiple-sequence alignment of ranavirus-encoded viral Bcl-2 (vBcl-2) homologs. Amino acid sequences of FV3 97R (AAT09757.1) and TFV 104R (ABB92349.1) were aligned using Clustal Omega. Highly conserved residues are highlighted in orange, while amino acid substitutions showing less functionally conserved positions are highlighted in blue. Gaps (–) indicate insertions or deletions introduced to optimize the alignment. The region highlighted in green shows significant variations in the C-terminal transmembrane region. (B) shows a BLASTP alignment depicting regions of sequence similarity between the FV3 97R gene (Query: AAT09757.1) and the anti-apoptotic protein Mcl-1 from *Xenopus laevis* (Subject: NP_001131055.1). The aligned region encompasses 36 amino acids and demonstrates 33% identity and 50% similarity, with an E-value of 9e-06, indicating a highly statistically significant match. Identical residues are displayed directly, while chemically similar amino acids are denoted by plus signs (+). The region highlighted in orange shows the predicted BH1 domain in 97R, which exhibits sequence similarity to the BH1 domain of Mcl-1. (C) shows the linear representation of the 97R amino acid sequence, highlighting key structural domains. The BH1 domain (residues 52-70) and the BH2 domain (residues 103–116) are indicated in orange, while the transmembrane domain (residues 118–137) is shown in purple. The amino acids (residues 1-112) marked with a green underline were used in the Yeast Two-Hybrid screening.

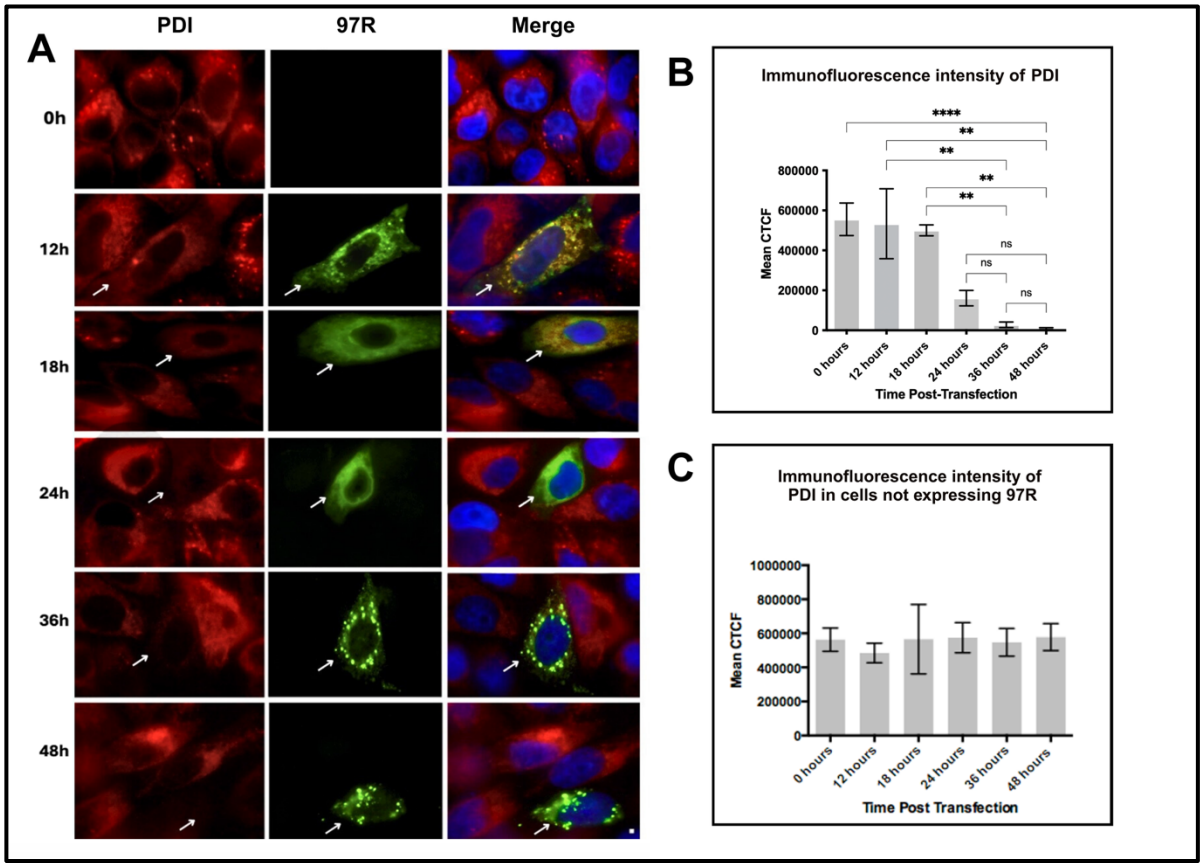

Figure 2.2. Time-dependent decrease in PDI expression following 97R transfection. (A) HeLa cells were transfected with Myc-Co97R and fixed at 0, 12, 18, 24, 36, and 48 h post-transfection. Indirect immunofluorescence was performed to detect 97R (anti-Myc; green), PDI (anti-PDI; red), and nuclei (DAPI; blue). Images were acquired using a Leica fluorescence microscope at 100X oil immersion. (B) PDI fluorescence intensity was quantified in 40 cells showing 97R expression per time point using ImageJ. (C) PDI fluorescence intensity was quantified in cells that did not express 97R at different time points. Error bars represent the mean ± S.D. (n = 3). Statistical analysis was performed using one-way ANOVA with Tukey's multiple comparisons post hoc test. Statistical significance: ns (non-significant), ** ($p < 0.01$), **** ($p < 0.0001$).

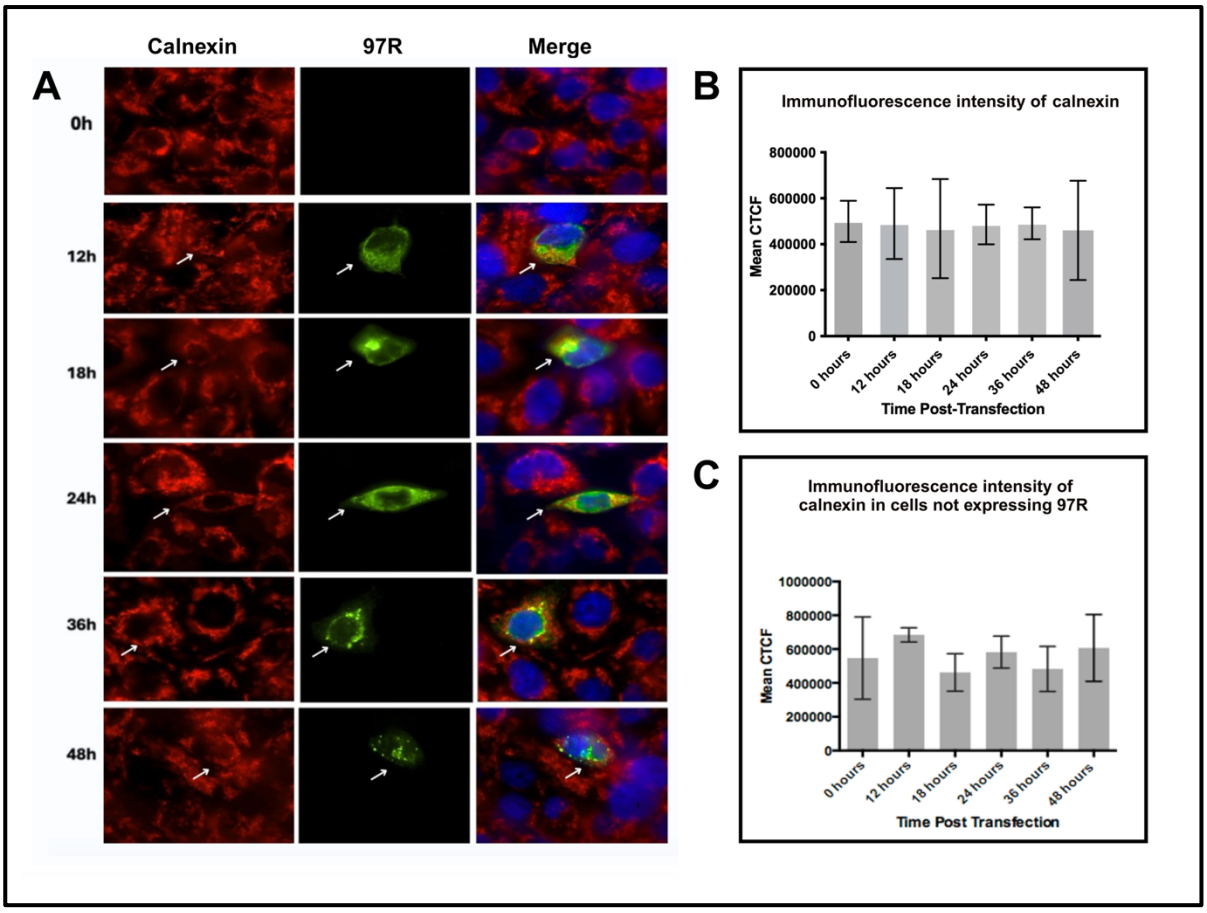

Figure 2.3. FV3 97R expression does not affect calnexin levels in the ER membrane. (A) HeLa cells were transfected with Myc-Co97R and fixed at 0, 12, 18, 24, 36, and 48 hours post-transfection. Indirect immunofluorescence was performed to detect 97R (anti-Myc; green), calnexin (anti-calnexin; red), and nuclei (DAPI; blue). Images were acquired at 100X oil immersion using the Leica fluorescence microscope. (B) Calnexin fluorescence intensity was quantified in 40 cells showing 97R expression per time point using ImageJ, and statistical analysis was performed using one-way ANOVA with Tukey's multiple comparisons post hoc test. (C) Calnexin fluorescence intensity was quantified in 40 cells that did not express 97R at different time points. Error bars represent the mean ± S.D. (n = 3).

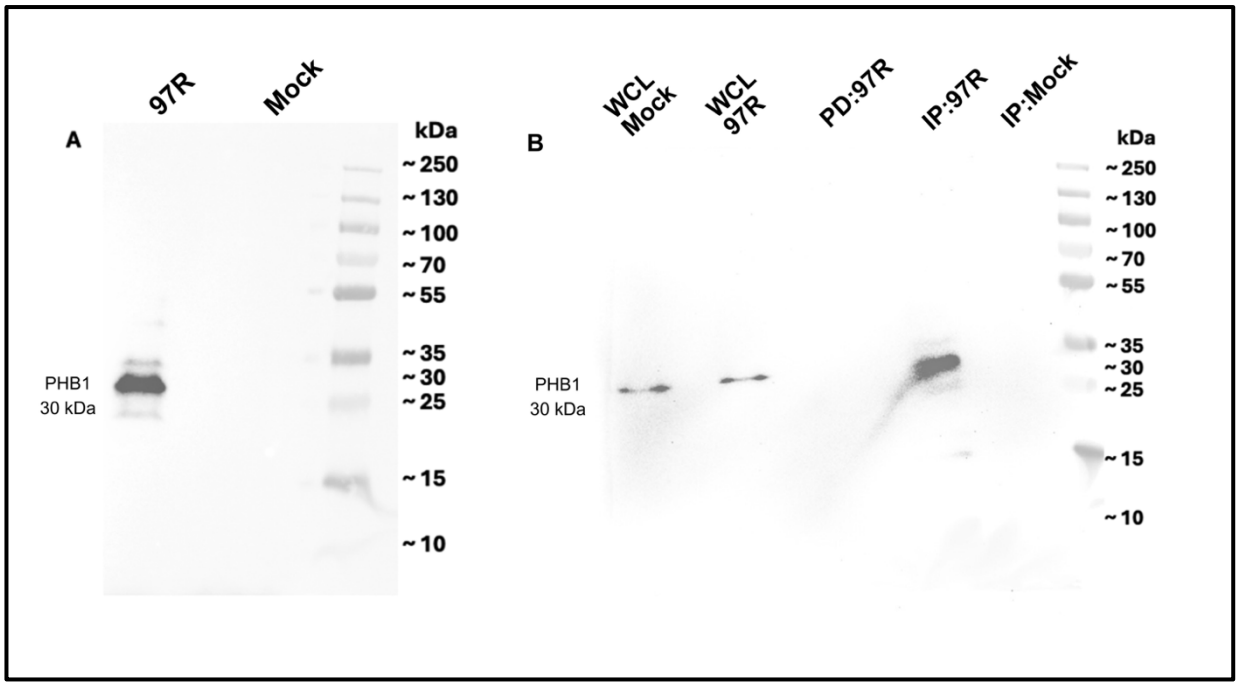

Figure 2.4. Immunoprecipitation (IP) and Western blot (WB) analysis of FV3 97R and PHB1 interaction in HeLa cells. HeLa cells were transfected with Myc-Co97R or mock-transfected. At 24 hours post-transfection, whole-cell lysates were prepared for IP and WB analysis. Lysates were immunoprecipitated with anti-Myc antibody and probed with anti-PHB1 antibody. (A) Immunoprecipitation (IP) samples from mock-transfected and 97R-transfected cells; PHB1 is detected only in the 97R-transfected IP lane. (B) Experimental replicate of (A); Western blot showing PHB1 in 97R-transfected IP lane, 97R-transfected whole cell lysate (WCL) lane and mock-transfected whole cell lysate (WCL) lane. No PHB1 detected in the mock-transfected IP lane and protein-depleted (PD) sample. Molecular weight markers are shown in kilodaltons (kDa) on the right.

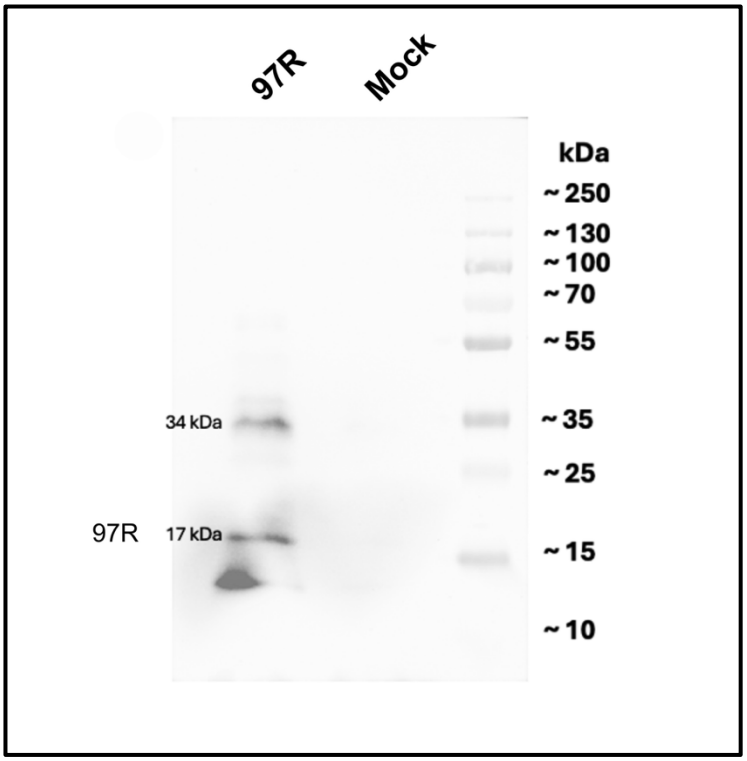

Figure 2.5. Reverse Immunoprecipitation (IP) and Western blot (WB) analysis of FV3 97R and PHB1 interaction in HeLa cells. HeLa cells were transfected with Myc-Co97R or mock-transfected. At 24 hours post-transfection, whole-cell lysates were prepared for IP and WB analysis. Lysates were immunoprecipitated with anti-PHB1 antibody and probed with anti-Myc antibody. 97R (at 17kDa) was detected in the 97R-transfected lane, which was immunoprecipitated with anti-PHB1 antibody. The 34kDa band represent a potential dimer of 97R. Molecular weight markers are shown in kilodaltons (kDa) on the right.

References:

1. Price SJ, Ariel E, Maclaine A, Rosa GM, Gray MJ, Brunner JL, et al. From fish to frogs and beyond: Impact and host range of emergent ranaviruses. *Virology*. 2017;511:272–9. doi:10.1016/j.virol.2017.08.001.

2. Chinchar VG, Yu KH, Jancovich JK. The molecular biology of Frog Virus 3 and other iridoviruses infecting cold-blooded vertebrates. *Viruses*. 2011;3(10):1959–85. doi:10.3390/v3101959.

3. Herath J, Sun D, Ellepola G, Subramaniam K, Meegaskumbura M. Emerging threat of ranavirus: Prevalence, genetic diversity, and climatic drivers of ranavirus (Iridoviridae) in ectothermic vertebrates of Asia. *Front Vet Sci*. 2023;10:1291872. doi:10.3389/fvets.2023.1291872.

4. Tan WGH, Barkman TJ, Chinchar VG, Essani K. Comparative genomic analyses of frog virus 3, type species of the genus Ranavirus (family Iridoviridae). *Virology*. 2004;323(1):70–84. doi:10.1016/j.virol.2004.02.019.

5. Neumann S, El Maadidi S, Faletti L, Haun F, Labib S, Schejtman A, et al. How do viruses control mitochondria-mediated apoptosis? *Virus Res*. 2015;209:45–55. doi:10.1016/j.virusres.2015.02.026.

6. Thomson BJ. Viruses and apoptosis. *Int J Exp Pathol*. 2001;82(2):65–76. doi:10.1046/j.1365-2613.2001.00195.x.

7. Cuconati A, White E. Viral homologs of bcl-2: Role of apoptosis in the regulation of virus infection. *Genes Dev*. 2002;16(19):2465–78. doi:10.1101/gad.1012702.

8. Lin J. A protein bridge to death between the ER and mitochondria. *J Biol Chem*. 2023;299(4):104581. doi:10.1016/j.jbc.2023.104581.

9. Ring BA, Lacerda AF, Drummond DJ, Wangen C, Eaton HE, Brunetti CR. Frog Virus 3 Open reading frame 97R localizes to the endoplasmic reticulum and induces nuclear invaginations. *J Virol*. 2013;87(16):9199–207. doi:10.1128/jvi.00637-13.

10. Banta KL, Wang X, Das P, Winoto A. B cell lymphoma 2 (bcl-2) residues essential for bcl-2's apoptosis-inducing interaction with NUR77/NOR-1 orphan steroid receptors. *J Biol Chem*. 2018;293(13):4724–34. doi:10.1074/jbc.ra117.001101.

11. Sancho M, Leiva D, Lucendo E, Orzáez M. Understanding MCL1: From cellular function and regulation to pharmacological inhibition. *FEBS J*. 2021;289(20):6209–36. doi:10.1111/febs.16136.

12. Brunelle JK, Letai A. Control of mitochondrial apoptosis by the Bcl-2 family. *J Cell Sci*. 2009;122(4):437–41. doi:10.1242/jcs.031682.

13. Postigo A, Eitz Ferrer P. Viral inhibitors reveal overlapping themes in regulation of cell death and innate immunity. *Microbes Infect*. 2009;11(13):1071–8. doi:10.1016/j.micinf.2009.08.012.

14. He J, Mi S, Qin XW, Weng SP, Guo CJ, He JG. Tiger frog virus ORF104R interacts with cellular VDAC2 to inhibit cell apoptosis. *Fish Shellfish Immunol*. 2019;92:889–96. doi:10.1016/j.fsi.2019.07.017.

15. Banjara S, Mao J, Ryan TM, Caria S, Kvansakul M. Grouper iridovirus GIV66 is a Bcl-2 protein that inhibits apoptosis by exclusively sequestering Bim. *J Biol Chem*. 2018;293(15):5464–77. doi:10.1074/jbc.ra117.000591.

16. Camacho C, Coulouris G, Avagyan V, Ma N, Papadopoulos J, Bealer K, et al. BLAST+: architecture and applications. *BMC Bioinformatics*. 2009;10:421. doi:10.1186/1471-2105-10-421.

17. Blum M, Andreeva A, Florentino LC, Chuguransky SR, Grego T, Hobbs E, et al. InterPro: The protein sequence classification resource in 2025. *Nucleic Acids Res*. 2024;53(D1):1082. doi:10.1093/nar/gkae1082.

18. Widden H, Placzek WJ. The multiple mechanisms of MCL1 in the regulation of cell fate. *Commun Biol*. 2021;4(1):1029. doi:10.1038/s42003-021-02564-6.

19. Sievers F, Wilm A, Dineen D, Gibson TJ, Karplus K, Li W, et al. Fast, scalable generation of high-quality protein multiple sequence alignments using Clustal Omega. *Mol Syst Biol*. 2011;7(1):539. doi:10.1038/msb.2011.75.

20. Goujon M, McWilliam H, Li W, Valentin F, Squizzato S, Paern J, et al. A new bioinformatics analysis tools framework at EMBL-EBI. *Nucleic Acids Res*. 2010;38(Web Server):W695–W699. doi:10.1093/nar/gkq313.

21. Zhao G, Lu H, Li C. Proapoptotic activities of protein disulfide isomerase (PDI) and PDIA3 protein, a role of the BCL-2 protein Bak. *J Biol Chem*. 2015 Apr 3;290(14):8949–63. doi: 10.1074/jbc.m114.619353.

22. Oliver JD, Hresko RC, Mueckler M, High S. The Glut 1 glucose transporter interacts with calnexin and calreticulin. *J Biol Chem*. 1996 Jun 7;271(23):13691–6. doi: 10.1074/jbc.271.23.13691.

23. Kersteen EA, Raines RT. Catalysis of protein folding by protein disulfide isomerase and small-molecule mimics. *Antioxid Redox Signal*. 2003;5(4):413–424. doi:10.1089/152308603768295159

24. Powell LE, Foster PA. Protein disulphide isomerase inhibition as a potential cancer therapeutic strategy. *Cancer Med*. 2021;10(8):2812–2825. doi:10.1002/cam4.3836

25. Perri ER, Thomas CJ, Parakh S, Spencer DM, Atkin JD. The unfolded protein response and the role of protein disulfide isomerase in neurodegeneration. *Front Cell Dev Biol*. 2016;3:80. doi:10.3389/fcell.2015.00080

26. Gallina A, Hanley TM, Mandel R, Trahey M, Broder CC, Viglianti GA, Ryser HJ. Inhibitors of protein-disulfide isomerase prevent cleavage of disulfide bonds in receptor-bound glycoprotein 120 and prevent HIV-1 entry. *J Biol Chem*. 2002;277(52):50579–50588. doi:10.1074/jbc.M204547200

27. Elliott T, Neefjes J. The complex route to MHC class I-peptide complexes. *Cell*. 2006;127(2):249–251. doi:10.1016/j.cell.2006.10.001

28. Antoniou AN, Powis SJ. Pathogen evasion strategies for the major histocompatibility complex class I assembly pathway. *Immunology*. 2008;124(1):1–12. doi:10.1111/j.1365-2567.2008.02804.x

29. Peng YT, Chen P, Ouyang RY, Song L. Multifaceted role of prohibitin in cell survival and apoptosis. *Apoptosis*. 2015;20(9):1135–1149. doi:10.1007/s10495-015-1143-z

30. Yurugi H, Tanida S, Ishida A, Akita K, Toda M, Inoue M, Nakada H. Expression of prohibitins on the surface of activated T cells. *Biochem Biophys Res Commun*. 2012;420(2):275–280. doi:10.1016/j.bbrc.2012.02.149

31. Chowdhury I, Thompson WE, Welch C, Thomas K, Matthews R. Prohibitin (PHB) inhibits apoptosis in rat granulosa cells (GCs) through the extracellular signal-regulated kinase 1/2 (ERK1/2) and the BCL family of proteins. *Apoptosis*. 2013;18(12):1513–1525. doi:10.1007/s10495-013-0901-z

CHAPTER 3

GENERAL DISCUSSION

In this study, we aimed to understand how the FV3-encoded 97R protein affects host cells, especially its influence on endoplasmic reticulum (ER) proteins, as viruses frequently exploit ER proteins to facilitate various stages of infection, including entry, protein synthesis, genome replication, assembly, and release (Woo et al., 2023). One of the most notable findings was the gradual, time-dependent decrease in protein disulfide isomerase (PDI) levels observed in HeLa cells transfected with the FV3 97R. PDI is a multifunctional 57 kDa chaperone that plays a key role in protein folding by catalyzing the formation and rearrangement of disulfide bonds between cysteine residues in proteins in the endoplasmic reticulum (ER) (Kersteen & Raines, 2003; Powell & Foster, 2021). Chaperones maintain proteins in a soluble state, allowing them to fold into their native conformations properly (Perri et al., 2016). In addition to its role in protein folding, PDI is also involved in regulating the ER stress response. PDI helps regulate the ER stress response by interacting with misfolded proteins to prevent aggregation and facilitate their degradation (Perri et al., 2016). The b' domain of PDI serves as the primary substrate-binding site, using hydrophobic interactions to confer high affinity and broad specificity (Perri et al., 2016). Since PDI is a vital chaperone involved in ensuring proper protein folding and maintaining ER homeostasis (Hetz et al., 2020), its downregulation in the cells transfected with 97R could impair ER function and disrupt cellular proteostasis. Impaired ER function could alter key signaling pathways activated in response to ER stress, including those that regulate apoptosis.

PDI is a well-established downstream target of the Activating Transcription Factor 6 (ATF6) pathway, a key branch of the unfolded protein response (UPR) activated during ER stress (Hetz et al., 2020). Under normal conditions, PDI is constitutively expressed in the endoplasmic reticulum (ER) of host cells, as part of the protein folding machinery (Perri et al., 2016). However, during ER stress, activation of the ATF6 pathway leads to the upregulation of PDI levels, which enhances the ER's folding capacity and ensures strict protein quality control by catalyzing disulfide bond formation and rearrangement (Hetz et al., 2020; Hillary & FitzGerald, 2018). This increase in PDI expression reflects the cell's adaptive response aimed at alleviating ER stress and restoring homeostasis. However, if ER stress remains unresolved and PDI stays elevated beyond its threshold, it could lead the host cell towards apoptosis. Therefore, the downregulation of PDI observed in 97R-expressing cells likely indicates a viral strategy to delay or inhibit apoptosis by disrupting the ER stress pathway. This disruption could benefit the virus, as it would prevent the host cell from undergoing apoptosis and allow FV3 to continue using the ER for its protein synthesis.

The PDI family members, beyond their traditional roles in protein folding, also actively participate in apoptosis. Previous research has shown that PDI can promote cell death by initiating Bak-dependent mitochondrial outer membrane permeabilization, which results in cytochrome c release and caspase activation, a hallmark of intrinsic apoptosis (Zhao et al., 2015). Inhibition of PDI has been shown to diminish apoptosis, suggesting that PDI also acts as a proapoptotic mediator (Zhao et al., 2015). Therefore, the observed decrease in PDI expression in 97R-expressing cells may also impair apoptotic signaling. To investigate whether 97R-induced PDI downregulation modulates

ER stress-mediated apoptotic signaling, further experiments should examine markers associated with ER stress-induced apoptosis. A previous study on Alzheimer's disease demonstrated through Western blot that ER stress-induced apoptosis involves the upregulation of C/EBP Homologous Protein (CHOP) and the cleavage of caspase-3, caspase-4, and caspase-12, which are markers of ER stress-induced apoptosis (Lee et al., 2010). Using a similar approach, future studies could involve Western blotting to determine the relative protein levels of CHOP and cleaved caspases in 97R-transfected cells and mock-transfected cells. A decrease in these markers would suggest that 97R inhibits the progression toward ER stress-induced apoptosis. To determine whether this effect is directly attributable to PDI downregulation due to 97R, cells could be engineered to overexpress PDI. PDI overexpression can be achieved by transfecting cells with a plasmid encoding PDI. This approach is similar to that employed by Wang et al. (2022) in colorectal cancer models, where the researchers developed PDI overexpression cell lines in HCT116, MEF, and A549 cells. Co-transfecting cells with 97R and a plasmid encoding PDI to restore PDI expression would help in the assessment of whether restored PDI levels alter the expression of apoptotic markers. Western blot analysis of CHOP and cleaved caspases in these co-transfected cells compared to 97R-only and mock controls would confirm the role of PDI in modulating ER stress-induced apoptosis after 97R expression. An increase in ER stress and apoptotic markers upon PDI overexpression in the presence of 97R would suggest that 97R’s downregulation of PDI is critical for suppressing ER stress-induced apoptosis. Collectively, these experiments could provide mechanistic insight into how 97R-mediated PDI downregulation may inhibit ER stress-

induced apoptotic signaling, potentially creating a cellular environment favourable for viral replication.

Several viruses are known to manipulate PDI to alter host cell functions in favour of viral replication or immune evasion (Gallina et al., 2002; Elliott & Neefjes, 2006). For example, human cytomegalovirus (CMV) expresses the US3 protein, which promotes the degradation of PDI and impairs the proper folding and surface expression of MHC class I molecules, allowing immune escape (Elliott & Neefjes, 2006). Similarly, our observation that FV3 97R leads to a significant downregulation of PDI could reflect a comparable viral strategy. By decreasing PDI levels, FV3 97R might disrupt UPR pathways, resulting in a failure of immune activation and thereby creating a more permissive environment for viral replication. Previous research has shown that unfolded protein response (UPR) triggered during ER stress can activate innate immune responses by inducing the production of pro-inflammatory cytokines such as interleukins IL-1, IL-6, and tumour necrosis factor-alpha (TNF-α) (Sprooten & Garg, 2020).To assess whether 97R-induced downregulation of PDI contributes to failure of immune activation, an enzyme-linked immunosorbent assay (ELISA) can be used to quantify cytokine secretion. Specifically, IL-1, IL-6, and TNF-α levels can be measured in the culture supernatants of cells transfected with 97R, mock-transfected controls, and cells co-transfected with 97R and a PDI overexpression construct. A reduction in cytokine secretion in 97R-transfected cells would suggest suppression of immune signaling potentially linked to ER stress dysfunction. Restoration of cytokine levels in cells co-transfected with PDI would support the hypothesis that 97R disrupts immune function and creates a favourable environment for viral replication.

Further mechanistic insights were gained from our yeast two-hybrid screen (Y2H), which identified prohibitin 1 (PHB1) as a potential interacting partner of 97R. We validated this interaction in HeLa cells using immunoprecipitation and Western blotting. Based on my results, FV3 97R appears to interact with prohibitin, an apoptotic regulator. While my research shows protein-protein interaction between PHB1 and 97R, how PHB1 contributes to FV3 infections remains unclear. PHB1 is a multifunctional protein primarily localized to mitochondria, but it is also found in the nucleus and plasma membrane (Peng et al., 2015). PHB1 inhibits apoptosis in rat granulosa cells, and overexpression of PHB1 increases the level of anti-apoptotic Bcl-2 family members, Bcl-2 and Bcl-XL, reducing the mitochondrial release of pro-apoptotic cytochrome c and inhibiting the activity of caspase-3 (Chowdhury et al., 2013). Therefore, PHB1 plays a vital role in promoting the expression of anti-apoptotic genes such as Bcl-2 and Bcl-XL, inhibiting caspase-3 activation, inhibiting apoptosis, thereby maintaining mitochondrial integrity (Chowdhury et al., 2013; Peng et al., 2015). Notably, another study has shown that overexpression of PHB in SH-SY5Y cells is sufficient to suppress the expression of ER stress markers, including Binding immunoglobulin Protein (BiP) and CHOP, highlighting PHB's role in maintaining mitochondrial and ER homeostasis (Wang et al., 2021). Additionally, PHB1 has been observed in mitochondria-associated membranes (MAMs) fractions (Sánchez-Vera et al., 2023) and implicated in processes such as mitochondrial integrity and ER stress regulation, which are functionally coordinated at mitochondria ER contact sites (MERCs) (Wang et al., 2021; C. Chen et al., 2024). Viral proteins from human herpesvirus (HCMV) and a hepacivirus (HCV) have been shown to move from the ER to mitochondria through MAMs (Williamson & Colberg-Poley, 2009).

At these ER-mitochondria contact sites, they regulate calcium (Ca^{2+}) signaling and apoptotic pathways, helping the virus delay cell death (Williamson & Colberg-Poley, 2009). Since 97R binds to PHB1, a mitochondrial stress-protective protein, it is possible that this interaction takes place through ER-mitochondria contact sites. By interacting with PHB1, 97R may manipulate mitochondrial dynamics and delay apoptosis, supporting viral survival and replication.

Interestingly, a recent study has shown that PHB2, a close homolog of PHB1, can interact with PDI to help regulate autophagy (Wang et al., 2022). ER stress typically activates the unfolded protein response (UPR), which, when sustained, triggers autophagy, a process where the cell breaks down its components (Kwon et al., 2023). This indicates a functional connection between prohibitins and PDI in stress response pathways. While my research focuses on PHB1, both PHB1 and PHB2 primarily perform functions together as heterodimers, particularly in mitochondrial regulation and cell survival (Nunes et al., 2021). The 97R-PHB1 interaction may affect PDI stability or expression, even without direct binding. Such a mechanism could be part of a broader viral strategy. By targeting PHB1 and indirectly influencing PDI, 97R may help the virus adjust the host's stress responses, extend cell survival to support viral replication, while gradually weakening the host cell's defence mechanism.

Evaluating whether PDI is similarly downregulated after FV3 infection is a crucial next step in this research. I transiently transfected HeLa cells with 97R for this study, but it is also important to assess PDI expression in cells infected with wild-type FV3 to determine if the virus uses 97R to regulate PDI during infection. Preliminary results indicate that FV3 infection causes significant cytopathic effects (data not shown).

Further research should explore whether these effects are connected to PDI depletion, which may shed light on how the virus affects host cell organelles. Time-course studies measuring PDI levels through immunofluorescence and Western blotting after FV3 infection would help understand PDI regulation and its role in viral replication during FV3 infection.

It is also important to acknowledge several limitations of this study. The absence of a 97R knockout FV3 strain prevents definitive conclusions about its role during natural FV3 infection. Further experiments utilizing a 97R-knockout virus could directly verify the role of 97R in PDI modulation during natural infection. This would help confirm whether 97R is directly responsible for the observed downregulation of PDI. Previous studies have shown successful creation of knockout FV3 (Chen et al., 2011; De Jesús Andino et al., 2015), and using the same strategy, a 97R-knockout FV3 could be generated by replacing the open reading frame (ORF) 97R with a Puro-EGFP cassette under a strong viral promoter, allowing both puromycin selection and fluorescent tracking of infected cells. A knock-in control virus, in which the cassette is inserted into a nonessential genomic region without disrupting 97R, would serve as a genetic control. HeLa cells could then be infected with wild-type FV3, 97R-knockout FV3 and knock-in control FV3, and PDI expression can be assessed at multiple time points. Western blotting would provide a quantitative measure of total PDI levels, while immunofluorescence microscopy would allow visualization of PDI localization and intensity changes in infected cells. If PDI downregulation is observed in wild-type and knock-in infections but not in 97R-knockout infections, this would confirm that 97R is necessary for PDI modulation during FV3 infection.

Our findings suggest that 97R may play a role in suppressing host cell apoptotic pathways by downregulating PDI, but further investigation is needed to confirm the role of 97R in the inhibition of apoptosis. To test whether 97R inhibits intrinsic apoptosis, cells could be transfected with a 97R-expressing plasmid alongside mock-transfected controls. After transfection, Western blotting could be used to examine key markers of the intrinsic apoptotic pathway. In particular, subcellular fractionation would enable detection of cytochrome c release from mitochondria into the cytosol by probing cytosolic fractions for cytochrome c protein levels (Ludovico et al., 2002). Additionally, Western blots could assess the levels of cleaved caspase-9 and caspase-3, which are downstream effectors of mitochondrial apoptosis. If 97R inhibits apoptosis, we would expect to observe decreased cytosolic cytochrome c and reduced levels of cleaved caspases in 97R-transfected cells compared to controls. This experimental approach offers a quantitative and specific way to evaluate the potential anti-apoptotic function of 97R. Another important question relates to the timing and progression of cellular stress responses induced by 97R. Time-course experiments should be performed, collecting samples at multiple time points post-transfection (e.g., 6, 12, 18, 24, 36, and 48 hours) to monitor the dynamics of unfolded protein response (UPR) activation and apoptosis induction. Western blotting for UPR markers such as BiP, alongside apoptotic markers like cleaved caspase-3, will clarify whether 97R expression delays or dampens ER stress-induced apoptotic signaling. Together, these studies will help determine if 97R acts as an inhibitor of intrinsic apoptosis and define the sequence of cellular stress events it triggers.

In conclusion, this research highlights how the FV3 97R protein may influence host cells by disrupting key stress response pathways in the endoplasmic reticulum (ER)

and mitochondria. We observed that 97R causes a gradual decrease in PDI, an essential protein for the proper folding of misfolded proteins in the ER and also interacts with PHB1. PHB1 helps regulate cell survival within the mitochondria. A graphical abstract of the findings from this research is presented in Figure 3.1. These findings indicate that 97R might assist the virus in keeping the host cell alive long enough to complete its replication by delaying stress responses and preventing cell death. Although we did not detect a direct interaction between 97R and PDI, the results suggest an indirect effect that may be connected to PHB1. This research advances our understanding of how FV3 alters host cells during infection. Building on these results, future studies should employ time-course experiments with a 97R-knockout virus to better understand how 97R regulates stress responses and PDI levels over time. In addition to shedding light on the functional role of FV3 97R in host cell modulation, these investigations offer new perspectives for understanding frog virus 3 better.

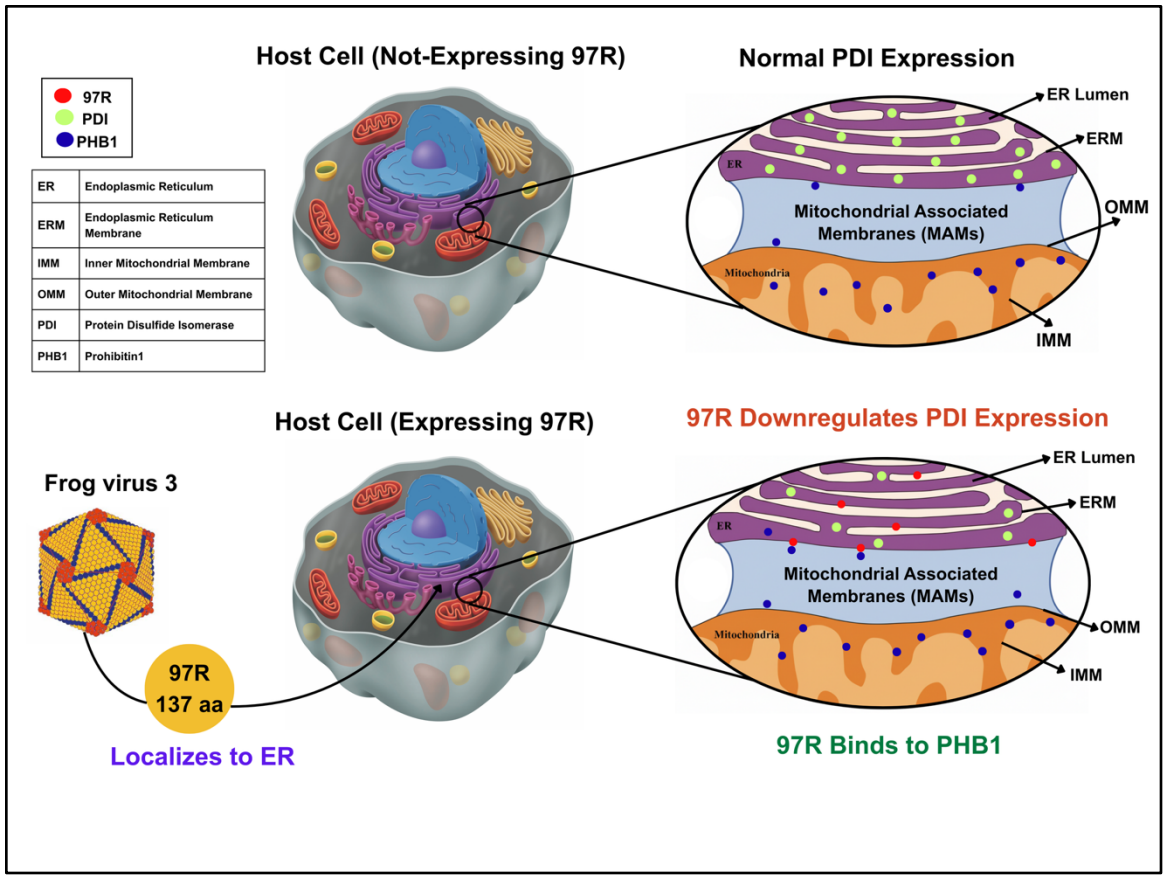

Figure 3.1. Graphical abstract. Figure created using Canva. This figure illustrates the role of frog virus 3 97R in host cells. In the cell that did not express 97R, Protein Disulphide Isomerase (PDI) expression remained unchanged, whereas in cells expressing 97R, PDI levels decreased significantly over time. Additionally, 97R also binds to Prohibitin 1 (PHB1) in the host cells.

References

Aniogo, E. C., George, B. P. A., & Abrahamse, H. (2020). Role of BCL-2 family proteins in photodynamic therapy mediated cell survival and regulation. *Molecules*, *25*(22), 5308. https://doi.org/10.3390/molecules25225308

Aviner, R., & Frydman, J. (2019). Proteostasis in Viral Infection: Unfolding the complex Virus–Chaperone Interplay. *Cold Spring Harbor Perspectives in Biology*, *12*(3), a034090. https://doi.org/10.1101/cshperspect.a034090

Banadyga, L., Veugelers, K., Campbell, S., & Barry, M. (2009). The Fowlpox Virus BCL-2 Homologue, FPV039, Interacts with Activated Bax and a Discrete Subset of BH3-Only Proteins To Inhibit Apoptosis. *Journal of Virology*, *83*(14), 7085–7098. https://doi.org/10.1128/jvi.00437-09

Bell, M. C., Meier, S. E., Ingram, A. L., & Abisambra, J. F. (2015). PERK-opathies: an endoplasmic reticulum stress mechanism underlying neurodegeneration. *Current Alzheimer Research*, *13*(2), 150–163. https://doi.org/10.2174/1567205013666151218145431

Borgese, N., Colombo, S., & Pedrazzini, E. (2003). The tale of tail-anchored proteins. *The Journal of Cell Biology*, *161*(6), 1013–1019. https://doi.org/10.1083/jcb.200303069

Boyce, M., & Yuan, J. (2006). Cellular response to endoplasmic reticulum stress: a matter of life or death. *Cell Death and Differentiation*, *13*(3), 363–373. https://doi.org/10.1038/sj.cdd.4401817

Brunelle, J. K., & Letai, A. (2009). Control of mitochondrial apoptosis by the Bcl-2 family. *Journal of Cell Science*, *122*(4), 437–441. https://doi.org/10.1242/jcs.031682

Camacho, C., Coulouris, G., Avagyan, V., Ma, N., Papadopoulos, J., Bealer, K., & Madden, T. L. (2009). BLAST+: architecture and applications. *BMC Bioinformatics*, *10*(1). https://doi.org/10.1186/1471-2105-10-421

Carstairs, S. J., Kyle, C. J., & Vilaça, S. T. (2020). High prevalence of subclinical frog virus 3 infection in freshwater turtles of Ontario, Canada. *Virology*, *543*, 76–83. https://doi.org/10.1016/j.virol.2020.01.016

Chen, C., Dong, X., Zhang, W., Chang, X., & Gao, W. (2024). Dialogue between mitochondria and endoplasmic reticulum-potential therapeutic targets for age-

related cardiovascular diseases. *Frontiers in Pharmacology*, *15*. https://doi.org/10.3389/fphar.2024.1389202

Chen, G., Ward, B. M., Yu, K. H., Chinchar, V. G., & Robert, J. (2011). Improved Knockout Methodology Reveals That Frog Virus 3 Mutants Lacking either the 18K Immediate-Early Gene or the Truncated vIF-2 α Gene Are Defective for Replication and Growth In Vivo. *Journal of Virology*, *85*(21), 11131–11138. https://doi.org/10.1128/jvi.05589-11

Chen, X., Shi, C., He, M., Xiong, S., & Xia, X. (2023). Endoplasmic reticulum stress: molecular mechanism and therapeutic targets. *Signal Transduction and Targeted Therapy*, *8*(1). https://doi.org/10.1038/s41392-023-01570-w

Chinchar, V. G., Yu, K. H., & Jancovich, J. K. (2011a). The Molecular Biology of Frog Virus 3 and other Iridoviruses Infecting Cold-Blooded Vertebrates. *Viruses*, *3*(10), 1959–1985. https://doi.org/10.3390/v3101959

Chowdhury, I., Thompson, W. E., Welch, C., Thomas, K., & Matthews, R. (2013). Prohibitin (PHB) inhibits apoptosis in rat granulosa cells (GCs) through the extracellular signal-regulated kinase 1/2 (ERK1/2) and the Bcl family of proteins. *APOPTOSIS*, *18*(12), 1513–1525. https://doi.org/10.1007/s10495-013-0901-z

Cuconati, A., & White, E. (2002). Viral homologs of BCL-2: role of apoptosis in the regulation of virus infection. *Genes & Development*, *16*(19), 2465–2478. https://doi.org/10.1101/gad.1012702

Daszak, P., Berger, L., Cunningham, A. A., Hyatt, A. D., Green, D. E., & Speare, R. (1999a). Emerging infectious diseases and amphibian population declines. *Emerging Infectious Diseases*, *5*(6), 735–748. https://doi.org/10.3201/eid0506.990601

De Jesús Andino, F., Grayfer, L., Chen, G., Chinchar, V. G., Edholm, E., & Robert, J. (2015). Characterization of Frog Virus 3 knockout mutants lacking putative virulence genes. *Virology*, *485*, 162–170. https://doi.org/10.1016/j.virol.2015.07.011

Elliott, T., & Neefjes, J. (2006). The complex route to MHC Class I-Peptide complexes. *Cell*, *127*(2), 249–251. https://doi.org/10.1016/j.cell.2006.10.001

Elmore, S. (2007). Apoptosis: A review of Programmed Cell Death. *Toxicologic Pathology*, *35*(4), 495–516. https://doi.org/10.1080/01926230701320337

Fu, X., Cui, J., Meng, X., Jiang, P., Zheng, Q., Zhao, W., & Chen, X. (2021). Endoplasmic reticulum stress, cell death and tumor: Association between endoplasmic reticulum stress and the apoptosis pathway in tumors (Review). *Oncology Reports*, *45*(3), 801–808. https://doi.org/10.3892/or.2021.7933

Gallina, A., Hanley, T. M., Mandel, R., Trahey, M., Broder, C. C., Viglianti, G. A., & Ryser, H. J. (2002). Inhibitors of Protein-Disulfide isomerase prevent cleavage of disulfide bonds in receptor-bound glycoprotein 120 and prevent HIV-1 entry. *Journal of Biological Chemistry*, *277*(52), 50579–50588. https://doi.org/10.1074/jbc.m204547200

Granoff, A., Came, P. E., & Breeze, D. C. (1966). Viruses and renal carcinoma of Rana pipiens. *Virology*, *29*(1), 133–148. https://doi.org/10.1016/0042-6822(66)90203-0

Hetz, C., Zhang, K., & Kaufman, R. J. (2020). Mechanisms, regulation and functions of the unfolded protein response. *Nature Reviews Molecular Cell Biology*, *21*(8), 421–438. https://doi.org/10.1038/s41580-020-0250-z

Hillary, R. F., & FitzGerald, U. (2018). A lifetime of stress: ATF6 in development and homeostasis. *Journal of Biomedical Science*, *25*(1). https://doi.org/10.1186/s12929-018-0453-1

Horimoto, S., Ninagawa, S., Okada, T., Koba, H., Sugimoto, T., Kamiya, Y., Kato, K., Takeda, S., & Mori, K. (2013). The unfolded protein Response transducer ATF6 represents a novel transmembrane-type endoplasmic reticulum-associated degradation substrate requiring both mannose trimming and SEL1L protein. *Journal of Biological Chemistry*, *288*(44), 31517–31527. https://doi.org/10.1074/jbc.m113.476010

Ishikawa, T., Kashima, M., Nagano, A. J., Ishikawa-Fujiwara, T., Kamei, Y., Todo, T., & Mori, K. (2017). Unfolded protein response transducer IRE1-mediated signaling independent of XBP1 mRNA splicing is not required for growth and development of medaka fish. *eLife*, *6*. https://doi.org/10.7554/elife.26845

Jeong, S., & Seol, D. (2008). The role of mitochondria in apoptosis. *BMB Reports*, *41*(1), 11–22. https://doi.org/10.5483/bmbrep.2008.41.1.011

Kelekar, A., & Thompson, C. B. (1998). Bcl-2-family proteins: the role of the BH3 domain in apoptosis. *Trends in Cell Biology*, *8*(8), 324–330. https://doi.org/10.1016/s0962-8924(98)01321-x

Kersteen, E. A., & Raines, R. T. (2003). Catalysis of protein folding by protein disulfide isomerase and Small-Molecule mimics. *Antioxidants and Redox Signaling*, *5*(4), 413–424. https://doi.org/10.1089/152308603768295159

Koyama, A., Fukumori, T., Fujita, M., Irie, H., & Adachi, A. (2000). Physiological significance of apoptosis in animal virus infection. *Microbes and Infection*, *2*(9), 1111–1117. https://doi.org/10.1016/s1286-4579(00)01265-x

Kwon, J., Kim, J., & Kim, K. I. (2023). Crosstalk between endoplasmic reticulum stress response and autophagy in human diseases. *Animal Cells and Systems*, *27*(1), 29–37. https://doi.org/10.1080/19768354.2023.2181217

Lee, J. H., Won, S. M., Suh, J., Son, S. J., Moon, G. J., Park, U., & Gwag, B. J. (2010). Induction of the unfolded protein response and cell death pathway in Alzheimer's disease, but not in aged Tg2576 mice. *Experimental & Molecular Medicine*, *42*(5), 386. https://doi.org/10.3858/emm.2010.42.5.040

Ludovico, P., Rodrigues, F., Almeida, A., Silva, M. T., Barrientos, A., & Côrte-Real, M. (2002). Cytochrome c Release and Mitochondria Involvement in Programmed Cell Death Induced by Acetic Acid in Saccharomyces cerevisiae. *Molecular Biology of the Cell*, *13*(8), 2598–2606. https://doi.org/10.1091/mbc.e01-12-0161

Ludwig, S., Planz, O., Pleschka, S., & Wolff, T. (2003). Influenza-virus-induced signaling cascades: targets for antiviral therapy? *Trends in Molecular Medicine*, *9*(2), 46–52. https://doi.org/10.1016/s1471-4914(02)00010-2

Marques, M., Ramos, B., Albuquerque, H., Pereira, M., Ribeiro, D. R., Nunes, A., Sarabando, J., Brás, D., Ferreira, A. R., Vitorino, R., Amorim, M. J., Silva, A. M., Soares, A. R., & Ribeiro, D. (2024). Influenza A virus propagation requires the activation of the unfolded protein response and the accumulation of insoluble protein aggregates. *iScience*, *27*(3), 109100. https://doi.org/10.1016/j.isci.2024.109100

Mazzoni, R., De Mesquita, A., Fleury, L., Brito, W., Nunes, I., Robert, J., Morales, H., Coelho, A., Barthasson, D., Galli, L., & Catroxo, M. (2009). Mass mortality associated with a frog virus 3- like Ranavirus infection in farmed tadpoles Rana catesbeiana from Brazil. *Diseases of Aquatic Organisms*, *86*, 181–191. https://doi.org/10.3354/dao02096

Miller, D. L., Rajeev, S., Gray, M. J., & Baldwin, C. A. (2007). Frog virus 3 infection, cultured American bullfrogs. *Emerging Infectious Diseases*, *13*(2), 342–343. https://doi.org/10.3201/eid1302.061073

Morrison, E. A., Garner, S., Echaubard, P., Lesbarrères, D., Kyle, C. J., & Brunetti, C. R. (2014). Complete genome analysis of a frog virus 3 (FV3) isolate and sequence comparison with isolates of differing levels of virulence. *Virology Journal*, *11*(1). https://doi.org/10.1186/1743-422x-11-46

Nunes, G. D., Wilson, E. R., Marziali, L. N., Hurley, E., Silvestri, N., He, B., O'Malley, B. W., Beirowski, B., Poitelon, Y., Wrabetz, L., & Feltri, M. L. (2021). Prohibitin 1 is essential to preserve mitochondria and myelin integrity in Schwann cells. *Nature Communications*, *12*(1). https://doi.org/10.1038/s41467-021-23552-8

Pearman, P. B., Garner, T. W. J., Straub, M., & Greber, U. F. (2004). RESPONSE OF THE ITALIAN AGILE FROG (RANA LATASTEI) TO a RANAVIRUS, FROG VIRUS 3: A MODEL FOR VIRAL EMERGENCE IN NAÏVE POPULATIONS. *Journal of Wildlife Diseases*, *40*(4), 660–669. https://doi.org/10.7589/0090-3558-40.4.660

Peng, Y., Chen, P., Ouyang, R., & Song, L. (2015). Multifaceted role of prohibitin in cell survival and apoptosis. *APOPTOSIS*, *20*(9), 1135–1149. https://doi.org/10.1007/s10495-015-1143-z

Perri, E. R., Thomas, C. J., Parakh, S., Spencer, D. M., & Atkin, J. D. (2016). The unfolded protein response and the role of protein disulfide isomerase in neurodegeneration. *Frontiers in Cell and Developmental Biology*, *3*. https://doi.org/10.3389/fcell.2015.00080

Powell, L. E., & Foster, P. A. (2021). Protein disulphide isomerase inhibition as a potential cancer therapeutic strategy. *Cancer Medicine*, *10*(8), 2812–2825. https://doi.org/10.1002/cam4.3836

Prew, M. S., Adhikary, U., Choi, D. W., Portero, E. P., Paulo, J. A., Gowda, P., Budhraja, A., Opferman, J. T., Gygi, S. P., Danial, N. N., & Walensky, L. D. (2022). MCL-1 is a master regulator of cancer dependency on fatty acid oxidation. *Cell Reports*, *41*(1), 111445. https://doi.org/10.1016/j.celrep.2022.111445

Qian, S., Wei, Z., Yang, W., Huang, J., Yang, Y., & Wang, J. (2022). The role of BCL-2 family proteins in regulating apoptosis and cancer therapy. *Frontiers in Oncology*, *12*. https://doi.org/10.3389/fonc.2022.985363

Read, A., & Schröder, M. (2021). The Unfolded Protein Response: An overview. *Biology*, *10*(5), 384. https://doi.org/10.3390/biology10050384

Redza-Dutordoir, M., & Averill-Bates, D. A. (2016). Activation of apoptosis signaling pathways by reactive oxygen species. *Biochimica Et Biophysica Acta (BBA) - Molecular Cell Research*, *1863*(12), 2977–2992. https://doi.org/10.1016/j.bbamcr.2016.09.012

Ring, B. A., Lacerda, A. F., Drummond, D. J., Wangen, C., Eaton, H. E., & Brunetti, C. R. (2013a). Frog Virus 3 Open reading frame 97R localizes to the endoplasmic reticulum and induces nuclear invaginations. *Journal of Virology*, *87*(16), 9199–9207. https://doi.org/10.1128/jvi.00637-13

Sánchez-Vera, I., Núñez-Vázquez, S., Saura-Esteller, J., Cosialls, A. M., Heib, J., Rodríguez, P. N., Ghashghaei, O., Lavilla, R., Pons, G., Gil, J., & Iglesias-Serret, D. (2023). The Prohibitin-Binding Compound Fluorizoline Activates the Integrated Stress Response through the eIF2α Kinase HRI. *International Journal of Molecular Sciences*, *24*(9), 8064. https://doi.org/10.3390/ijms24098064

Schloegel, L., Daszak, P., Cunningham, A., Speare, R., & Hill, B. (2009). Two amphibian diseases, chytridiomycosis and ranaviral disease, are now globally notifiable to the World Organization for Animal Health (OIE): an assessment. *Diseases of Aquatic Organisms*, *92*(3), 101–108. https://doi.org/10.3354/dao02140

Singh, R., Letai, A., & Sarosiek, K. (2019). Regulation of apoptosis in health and disease: the balancing act of BCL-2 family proteins. *Nature Reviews Molecular Cell Biology*, *20*(3), 175–193. https://doi.org/10.1038/s41580-018-0089-8

Sprooten, J., & Garg, A. D. (2020). Type I interferons and endoplasmic reticulum stress in health and disease. *International Review of Cell and Molecular Biology*, 63–118. https://doi.org/10.1016/bs.ircmb.2019.10.004

Suraweera, C. D., Banjara, S., Hinds, M. G., & Kvansakul, M. (2022). Metazoans and Intrinsic apoptosis: An evolutionary analysis of the BCL-2 family. *International Journal of Molecular Sciences*, *23*(7), 3691. https://doi.org/10.3390/ijms23073691

Szegezdi, E., Logue, S. E., Gorman, A. M., & Samali, A. (2006). Mediators of endoplasmic reticulum stress-induced apoptosis. *EMBO Reports*, *7*(9), 880–885. https://doi.org/10.1038/sj.embor.7400779

Takizawa, T., Matsukawa, S., Higuchi, Y., Nakamura, S., Nakanishi, Y., & Fukuda, R. (1993). Induction of programmed cell death (apoptosis) by influenza virus

infection in tissue culture cells. *Journal of General Virology*, *74*(11), 2347–2355. https://doi.org/10.1099/0022-1317-74-11-2347

Tan, W. G., Barkman, T. J., Chinchar, V. G., & Essani, K. (2004a). Comparative genomic analyses of frog virus 3, type species of the genus Ranavirus (family Iridoviridae). *Virology*, *323*(1), 70–84. https://doi.org/10.1016/j.virol.2004.02.019

Wang, R., Shang, Y., Chen, B., Xu, F., Zhang, J., Zhang, Z., Zhao, X., Wan, X., Xu, A., Wu, L., & Zhao, G. (2022). Protein disulfide isomerase blocks the interaction of LC3II-PHB2 and promotes mTOR signaling to regulate autophagy and radio/chemo-sensitivity. *Cell Death and Disease*, *13*(10). https://doi.org/10.1038/s41419-022-05302-w

Wang, X., Ding, D., Wu, L., Jiang, T., Wu, C., Ge, Y., & Guo, X. (2021). PHB blocks endoplasmic reticulum stress and apoptosis induced by MPTP/MPP+ in PD models. *Journal of Chemical Neuroanatomy*, *113*, 101922. https://doi.org/10.1016/j.jchemneu.2021.101922

Warren, C. F. A., Wong-Brown, M. W., & Bowden, N. A. (2019). BCL-2 family isoforms in apoptosis and cancer. *Cell Death and Disease*, *10*(3). https://doi.org/10.1038/s41419-019-1407-6

Weston, R. T., & Puthalakath, H. (2010). Endoplasmic reticulum stress and BCL-2 family members. *Advances in Experimental Medicine and Biology*, 65–77. https://doi.org/10.1007/978-1-4419-6706-0_4

Williamson, C. D., & Colberg-Poley, A. M. (2009). Access of viral proteins to mitochondria via mitochondria-associated membranes. *Reviews in Medical Virology*, *19*(3), 147–164. https://doi.org/10.1002/rmv.611

Woo, T., Williams, J. M., & Tsai, B. (2023). How host ER membrane chaperones and morphogenic proteins support virus infection. *Journal of Cell Science*, *136*(13). https://doi.org/10.1242/jcs.261121

Wu, P., Zhang, X., Duan, D., & Zhao, L. (2023). Organelle-Specific Mechanisms in Crosstalk between Apoptosis and Ferroptosis. *Oxidative Medicine and Cellular Longevity*, *2023*, 1–14. https://doi.org/10.1155/2023/3400147

Yuen, C., Matsumoto, K., & Christopher, D. (2013). Variation in the Subcellular Localization and Protein Folding Activity among Arabidopsis thaliana Homologs of Protein Disulfide Isomerase. *Biomolecules*, *3*(4), 848–869. https://doi.org/10.3390/biom3040848

Zhao, G., Lu, H., & Li, C. (2015). Proapoptotic activities of protein disulfide isomerase (PDI) and PDIA3 protein, a role of the BCL-2 protein Bak. *Journal of Biological Chemistry*, *290*(14), 8949–8963. https://doi.org/10.1074/jbc.m114.619353